

LIBRARY
ROYAL AIR FORCE ESTABLISHMENT
BEDFORD.



MINISTRY OF DEFENCE (PROCUREMENT EXECUTIVE)

AERONAUTICAL RESEARCH COUNCIL

CURRENT PAPERS

Papers on Novel Aerodynamic
Noise Source Mechanisms
at Low Jet Speeds

By

*John E. Ffowcs Williams, F. G. Leppington,
D. G. Crighton and H. Levine*

LONDON · HER MAJESTY'S STATIONERY OFFICE

1972

Price £1.13 net

Papers on Novel Aerodynamic Noise Source Mechanisms
at Low Jet Speeds

- by -

John E. Ffowcs Williams
F. G. Leppington
D. G. Crighton
H. Levine

SUMMARY

This is a Current Paper combining five separate papers under the following headings:-

- (1) Sound Generation by Turbulence contained in a Small Vessel
- (2) Transmission of Low Frequency Jet Pipe Sound through a Nozzle Flow
- (3) Radiation Properties of the Semi-Infinite Vortex Sheet
- (4) Diffraction Radiation
- (5) Scattering of Quadrupole Sources near the End of a Rigid Semi-Infinite Circular Pipe

Both the long wave and short wave problems are discussed. There are several aspects of the problem that remain unsolved and further theoretical work should be encouraged.

Introduction

The noise of the early jet engines increased in proportion to the fourth power of velocity. In 1952 Mawardi and Dyer reported measurements on turbo-jet engine noise. The velocity index varied from 4 to 8 as the thrust was increased. In that year Lighthill's pioneering theory showed how turbulence in free space radiated sound in proportion to the eighth power of velocity; from that time on the low velocity behaviour seems to have been forgotten. It was regarded as an indication of rough burning, or some anomalous turbine noise, and was treated more as an imperfection of the machine rather than a fundamental effect. In laboratory studies also, many forms of rig noise had to be eliminated in calibration of the experiments. Gauzes and honeycombs were used to eliminate turbulence, and nozzles with extremely high contraction ratios were used to obtain smooth nozzle exit flow. The dependence of the noise on the eighth power of velocity was used as a check on the usability of the equipment. As time went on the noise of real engines scaled more and more like the eighth power of velocity as the specific thrust was increased and the performance was improved by eliminating internal losses which no doubt induced turbulence in the nozzle exit flow. In the Bakerian lecture Lighthill (1961) was able to point to the relevance of his theory to practical engines. There was only one aspect that was in any way unsatisfactory. The convective effects, so important in distributing preferentially the radiation in the direction of jet motion, also bring about an increased efficiency, so that the sound scales with a higher velocity index than 8. At 90° to the jet axis, where the convective effects are absent, an eighth power law is predicted. Experiments in fact show that a velocity index nearer 6 is measured at 90° and the overall power scales very closely on the eighth power of velocity. Lighthill drew attention to measurements of turbulence level which showed that the relative turbulence intensity tended to be a decreasing function of Mach number. He gave a very plausible argument that this decrease accounted for a reduction of the sound level which exactly compensated for the increased radiation efficiency brought about by the convective effects. The eighth power law still described the experiments but for a slightly different reason. This coincidence is a little unsatisfactory however since recent experiments carried out by Lush⁴ show that the frequencies, that are set by the turbulence level, increased linearly with velocity, and his exceptionally carefully prepared jet flow does show the increase in radiative power above the U^8 line. The sound intensity at 90° to the jet axis scales precisely with the eighth power of velocity in complete accord with Lighthill's theory. Modern engines run at lower jet speeds to achieve jet noise suppression. The achieved suppression is not as great as an eighth power law would imply. We are therefore led to the conclusion that the Lighthill model of free turbulence only partly describes the sound of real turbo-jet engines though it deals completely with a carefully prepared model problem. This failure of the model can be turned to a distinct advantage.

The U^8 law is a rigorous derivation from free quadrupole theory asymptotic for low Mach number. That the law fails at low Mach number is positive proof that the sources of low speed noise lie outside the Lighthill free turbulence model. The new noise sources that are now becoming important must be sought either within or at the nozzle surface. Curle (1955) showed that when boundaries are present monopoles arise at free surfaces and dipoles on rigid surfaces. An unsteady mass flow in the nozzle exit would radiate monopole sound and an unsteady jet thrust would radiate dipole sound,

both more efficient than the basic quadrupole mechanism. This was the model taken by Ffowcs Williams and Gordon⁶ who also showed experimentally that the non-U⁸ noise is an increasing function of internal jet pipe turbulence level. This first viewpoint is however too naive.

Unsteady mass flow from the engine, which tends to be large on a wavelength scale, is only permitted as a result of internal fluid dilatation, an effect which must vanish as the compressibility, or the Mach number, tends to zero. The monopole strength is consequently factored by a Mach number and the velocity index increased. A proper treatment of this problem must rest on the yet unexplored internal acoustics of a jet engine, (Ffowcs Williams 1970). A first step in this problem was taken by Davies and Ffowcs Williams¹⁴ in considering the problem of sound generation by turbulence contained within a long pipe. They showed a fundamental increase in the sound producing ability of confined turbulence providing that the acoustic wavelength was much larger than the pipe's diameter. However, this is precisely the condition required for inefficient radiation from the termination of the pipe so that this increased sound production would not be noticed in the jet exterior. Waves incident upon the nozzle exit would, in the main, be reflected back upstream. However, if there is an upstream obstruction which reflects upstream travelling waves back in the direction of the nozzle, then in the end the waves would get out but only at the discrete frequency characteristic of the organ pipe. This inability of sound generated efficiently within a jet pipe to escape into the environment was pointed out by Gordon and Maidanik⁸ and Heller and Widnall⁹.

That some new source must become dominant at low speeds is no surprise. Lighthill pointed out the extreme inefficiency of free quadrupoles as sources of sound. He argued that resonators could increase the acoustic output and that turbulence could interact with a mean shear layer using it as a sounding board to increase the sound power output. Solid surfaces could of course act as sounding boards. These suggestions have now to be taken more seriously since the 'new' sources are evidently controlling the sound radiation of modern turbo-jets with their relatively low exhaust speeds.

The refraction of sound as it travels from its turbulent origin through a mean shear flow is neglected in the Lighthill model. Lush⁴ has shown that this refraction is a controlling factor at near grazing incidence to the jet axis. At low angles the effect arrests the increase of frequency and intensity with speed. This refraction has been treated numerically by Schubert¹⁰ in a scheme which integrates the governing equations for a given jet profile. Schubert suppresses the instabilities that inevitably exist with an inflectional velocity profile - a step of yet undetermined relevance to the practical problem. Howe¹¹ treats analytically the geometrically simpler problem of sound sources close to a plain vortex sheet. He shows how the interaction between the sound and the flow is a dominant feature of the problem and how the instabilities control the process in the so-called zone of silence. The main features of interest in all these refractive interaction situations occur at angles within 90° of the jet axis. There is a minimum of effect at 90°. These interaction effects are also decreasing as the Mach number is reduced.

The main characteristic of the low speed problem is that non-U⁸ behaviour becomes increasingly important at low Mach numbers and the effect is most apparent at 90° to the jet axis. Whether this is on account of a preferential directivity in the 90° direction or simply because the U⁸

sources are weaker in this direction is not yet known. A simple minded survey of sound at one frequency in no way indicates the source properties since Doppler effects depend on radiation angle, and must be accounted for to select the field of any individual source. This point was used by Lush⁴ to great effect and his technique which exploited a thorough understanding of the basic physical processes with a critical experimental survey could well be used now to throw light on the low speed problem. This report aims to identify some of the important physical processes that might be examined in such an experimental programme.

The interaction of sound with the shear layer per se is evidently not a promising starting point to the search for the high efficiency low speed sources that are relevant to the practical problem. However, we shall conclude that the interaction of the shear layer with the nozzle surface is likely to be a powerful effect.

The most comprehensive experimental survey of low Mach number non-quadrupole sound that is so far available is due to Gordon and Maidanik⁸ and Heller and Widnall⁹ who study the additional noise made by a jet emerging from a pipe containing specific turbulence generators or spoilers. They actually measure the fluctuating forces on the spoilers and give a convincing interpretation of the dominant processes that operate in their experiment. Unfortunately the particular situation studied by them is proving quite different in character to the emerging problem of low speed jet engine noise, in that the velocity dependence and directionality are different. But then their experimental setup was quite different also. Their jet pipe was not fitted with a nozzle, so that the jet pipe velocity was uncharacteristically high. The nozzle itself may have a fundamental influence on noise. In fact it is quite unreasonable to expect their experiment to model an engine at all. Unreasonable also is the expectation that any rig survey of the low speed noise problem is in some way universal. The remarkable fact is that there does appear to be some evidence of a universal structure. Any universality in the low speed problem seems highly improbable because the low speed failure of Lighthill's free quadrupole model, and its precise asymptotic description, is positive proof that the low speed sources lie either within or at the nozzle exit. If the sources are at the exit plane then the turbulence there may be essentially driven from the unstable turbulent downstream shear layers. In that event some universal form is feasible. However if the sources are within the jet pipe where conditions vary enormously from one engine installation to the next, and certainly from engine to model rigs, a universal low speed non-U⁸ structure is quite out of the question. Nor can it seriously be suggested in the light of low speed jet experiments where there is in fact a prolific body of information available from the heating and ventilation field. Jet exhaust noise is there the limiting factor preventing the use of more economic smaller conduits conveying air at high speed.

At this time then, we seem to be concerned with the details of rig noise which the early experimentalists took such pains to eliminate. It obviously depends on the rig and its internal acoustics. It is becoming practically significant now because of reductions in the free turbulence noise that accompany a lowering in jet speeds and the development of more efficient jet suppressors. Actually, the problem is not really restricted to low speeds but to all jets where the Lighthill-type sources can be suppressed.

The previous comment that resonators can increase the acoustic radiation from turbulence has not been worked out in any quantitative way. This is done in Chapter 1 of this report and is thought to be relevant since the interior of an engine contains many resonant cavities. Specifically, the combustion chamber constitutes a Helmholtz resonator whose resonances are known to be troublesome in accounting for vibration that affects its structural integrity. It will be seen that the interior motion is also capable of generating sound very effectively and that turbulence and/or turbulent combustion is a possible source of low speed high amplitude noise. The jet pipe too is a resonator of the organ pipe variety, and high amplitude low frequency organ tones, which may well be termed 'howl', are likely to occur unless the modes are damped in some deliberate manner. These sounds would all scale on a velocity index lower than 8 provided only that the unsteady flows have a Strouhal frequency at, or above, the fundamental oscillator resonance frequency. These resonators generate sound in the manner of acoustic monopoles and scale on the third or fourth power of velocity depending on whether the radiation is at or above the resonance frequency. Also, surfaces can scatter hydrodynamic motion into sound. Small surfaces do this in the well documented way described by Curle (1955) while large surfaces do it in a basically more efficient manner that is less well understood and may depend on details of geometry. It is this problem that is treated most extensively in this report, the object being to describe the physical characteristics of sound generation in the neighbourhood of the nozzle exit when it is irradiated by turbulent sources in the presence of an evolving shear layer.

Chapter 2 deals with the low frequency behaviour of the jet pipe and nozzle configuration at low flow Mach numbers when the wavelength of the sound is large on the nozzle scale. The argument is made much more formal in a rigorous treatment that neglects the influence of mean flow and the presence of the nozzle in Chapter 5. There the diffraction of aerodynamic sources by a semi-infinite pipe is treated exactly. The relevance of this model problem to the practical situation rests entirely on Lighthill's exact acoustic analogy. The conclusions reached in these Chapters are that the turbulence in the vicinity of the nozzle exit will generate long wavelength sound that scales in proportion to the sixth power of velocity. Aerodynamic sources deep in the pipe will scale on velocity in precisely the same manner as they would in free space. At higher frequencies, when the wavelength is short on the scale of the nozzle diameter, sound escapes from the nozzle unimpeded so that again the containment of sources within the jet pipe cannot alter their velocity dependence. Also in this limit, the basic canonical problem neglects surface curvature and considers the sound generated by unsteady flow in the vicinity of a sharp edge to a semi-infinite bounding surface. This was done by Ffowcs Williams and Hall¹² who showed how sound was generated in a basically more efficient way by edge scattering, the acoustic intensity scaling on the fifth power of flow velocity. Crighton and Leppington¹³ showed how this argument could be generalised to different geometries with no essential modification of the conclusions. These arguments are taken much further in Chapter 3 of this report by including the interaction of the shear layer and the bounding surfaces and also including for the first time a non-trivial exact solution of the flow equations that incorporates various forms of a Kutta constraint. Sound is indeed generated very efficiently by the interaction, the efficiency increasing by a large amount as the Kutta condition is applied. In this category also, we consider edge-scattered sound from those parts of the turbulence that are silent in the absence of the edge. This is the case for slowly evolving eddies.

When these eddies are convected with the flow and emerge from the shadow of the boundary their steady field adjusts to the free space value. This adjustment is unsteady and produces a propagating sound that we term 'diffraction radiation'. That problem is treated in Chapter 4. Again the intensity is shown to scale on the fifth power of velocity. These edge-scattering mechanisms all generate sound that radiates preferentially away from the jet axis and at a frequency higher, by a factor of about 4, than the basic jet noise. It also scales with a velocity index equal to or less than 5. In this way it seems to describe many of the experimental features of the current practical low speed jet noise problem at sound wavelengths that are shorter than the nozzle scale.

The concluding Chapter describes what experimental checks might be made on the relevance of the theoretical model to the practical problem. It gives also some indication of problems that remain outstanding. These are both theoretical and experimental.

References/

References

<u>No.</u>	<u>Author(s)</u>	<u>Title, etc.</u>
1	O. K. Mawardi and I. Dyer	On noise of aerodynamic origin. J. Acoust. Soc. Am. <u>25</u> , No. 3. 1952.
2	M. J. Lighthill	On sound generated aerodynamically. Proc. Roy. Soc. (London) <u>A.211</u> , 1952.
3	M. J. Lighthill	Sound generated aerodynamically. The Bakerian Lecture. Proc. Roy. Soc. (London) <u>A.267</u> . 1961.
4	P. A. Lush	Measurements of subsonic jet noise and comparison with theory. J. Fluid Mech. <u>46</u> , 3. 1971.
5	N. Curle	The influence of solid boundaries upon aerodynamic sound. Proc. Roy. Soc. (London) <u>A.231</u> . 1955.
6	J. E. Ffowcs Williams and C. G. Gordon	Noise of highly turbulent jets at low exhaust speeds. A.I.A.A. Journal <u>3</u> , 4. 1965.
7	J. E. Ffowcs Williams	Aeronautical acoustics as a problem in Applied Mathematics. Imperial College of Science and Technology Inaugural Lectures. 1970.
8	C. G. Gordon and G. Maidanik	Influence of upstream flow discon- tinuities on the acoustic power radiated by a model air jet. N.A.S.A. CR-679. 1967.
9	H. H. Heller and S. E. Widnall	Sound radiation from rigid flow spoilers correlated with fluctuating forces. J. Acoust. Soc. Am. <u>47</u> , 3, Part 2. 1970.

References (Continued)

<u>No.</u>	<u>Author(s)</u>	<u>Title, etc.</u>
10	L. K. Schubert	Refraction of sound by a jet: A Numerical Study. U.T.I.A.S. Report No. <u>144</u> , 1969.
11	M. S. Howe	Transmission of an acoustic pulse through a plane vortex sheet. J. Fluid Mech. <u>43</u> , 2. 1970.
12	J. E. Ffowcs Williams and L. H. Hall	Aerodynamic sound generation by turbulent flow in the vicinity of a scattering half-plane. J. Fluid Mech. <u>40</u> , 4. 1970.
13	D. G. Crighton and F. G. Leppington	Scattering of aerodynamic noise by a semi-infinite compliant plate. J. Fluid Mech. <u>43</u> , 4. 1970.
14	H. G. Davies and J. E. Ffowcs Williams	Aerodynamic sound generation in a pipe. J. Fluid Mech. <u>32</u> , 4.

Chapter 1

Sound Generation by Turbulence contained in a Small Vessel

by

John E. Ffowcs Williams,
Department of Mathematics,
Imperial College, London

Some features of the jet engine noise problem at relatively low exhaust speeds, lead to the view that the unsteady turbulent flow within the combustion chambers may well be an important source of external noise. These flows are characteristically very hot, the local speed of sound is high, and many sounds of practical interest fall in the frequency range where the acoustic wavelength in the hot flow is larger than the linear dimension of the combustion chamber. The combustion chamber is then a 'small vessel' in the sense used here. Sound will not be a significant factor in the internal fluid motion of such a small vessel. We consider that the vessel, of internal volume V , communicates with the exterior homogeneous environment through a small fraction of its bounding surface, and for definiteness, we model the apertures as a single tubular 'neck' of length L and cross-sectional area A . The vessel constitutes a 'Helmholtz' resonator whose acoustical properties are easily described. Away from the resonance frequency sound is generated as a by-product of the mainflow and is of sufficiently small magnitude that it does not feature in the dynamical balance that constrains the internal motion. The sound can be determined from the motion at the 'neck' which acts on the environment like a monopole source of strength equal to the rate at which the mass flow leaving V is changing in time. At the resonance frequency, however, sound is the main loss term that limits the amplitude and it then features prominently in the balance by which the flow is determined.

We wish to determine the sound level that is generated exterior to the vessel by turbulence and turbulent combustion which we suppose to be contained in the vessel. We will consider first the non-resonant case and then examine separately the question of resonance frequency sound generation. The model problem is illustrated in Fig. 1.

Non-Resonant Behaviour

The pressure $p(t)$ at the entry to the neck can be decomposed into two components, one arising from the dilatation caused by one-dimensional motion in the neck, $p_v(t)$ say, and the other the pressure that would be at that position were the velocity at the neck externally restricted to zero $p_r(t)$.

$$p = p_v + p_r \quad \dots (1)$$

p_r is thus the pressure induced in a rigid walled unventilated vessel and may itself be attributed to two effects. Firstly, turbulence in the vessel will induce an unsteady pressure p_t whose magnitude will scale on the unsteady Reynolds stresses and whose frequency ω , will be determined by the Strouhal number based on the characteristic velocity and turbulence length scale in the vessel, U and ℓ respectively.

$$\begin{aligned} p_t &\sim \bar{\rho} U^2 \\ \omega &\sim U/\ell \end{aligned} \quad \dots (2)$$

$\bar{\rho}$ is the mean density within the vessel.

Secondly, unsteady heat addition will cause the pressure in the constant volume vessel to vary, and we will label this component of p_r as p_q .

$$p_r = p_t + p_q \quad \dots (3)$$

$$p_q = (\gamma - 1) \rho q \quad \dots (4)$$

where q is the average over the volume V of the unsteady component of heat addition per unit mass. This will typically be a small fraction α , say, of the steady heat addition per unit mass which in a jet engine is equal to the mechanical energy per unit mass in the exhaust flow, U_j^2 .

$$p_q = \alpha(\gamma - 1) \bar{\rho} U_j^2 ; \quad \dots (5)$$

The unsteady pressure p_t , for a given turbulence level in the chamber, will therefore scale on a mean velocity squared, the velocity being either the local chamber flow velocity or the mean jet velocity depending on whether the local inertial term or that arising from unsteady burning is dominant.

Unsteady flow out of the volume will introduce the additional pressure p_v . When the velocity in the neck is v the density in the vessel will be reducing at a rate $\frac{\bar{\rho} v A}{V}$, and the pressure at a rate c^2 times this.

$$\frac{\partial p_v}{\partial t} = \left(\frac{\bar{\rho} c^2 A}{V} \right) v . \quad \dots (6)$$

The fluid in the neck has an inertia which the difference in pressure between the vessel interior and the environment, $p - p_a$, must overcome.

$$(p - p_a) /$$

$$(p - p_a) = L\bar{\rho} \frac{\partial v}{\partial t} = p_r + p_v - p_a = p_r' - p_v \quad \dots (7)$$

The unsteadiness in ambient pressure p_a is absorbed into a re-defined p_r' since it is due predominantly to local hydrodynamic effects that are independent of any motion in the resonator neck. This is because at large wavelengths (compared to the dimension of the orifice) source motion is ineffective in generating changes in external pressure, and the small changes that are introduced are fully accounted for in a slight re-definition of neck length - which is in any event imperfectly modelled. The significance of absorbing the environmental changes into p_r' is that the step emphasises an essential point that hydrodynamic pressures interior or exterior to the resonator are scattered into sound in a precisely similar fashion with identical efficiencies.

Equations (6) and (7) can be combined to form an inhomogeneous oscillator equation that we write here in terms of the simple source

$$\text{strength } \bar{\rho} \frac{\partial v}{\partial t} \cdot A.$$

$$\left\{ \frac{\partial^2}{\partial t^2} + \omega_0^2 \right\} \bar{\rho} A \frac{\partial v}{\partial t} = \frac{A}{L} \frac{\partial^2 p_r'}{\partial t^2} \quad \dots (8)$$

where,

$$\omega_0 = c \sqrt{\frac{A}{VL}}.$$

ω_0 is the Helmholtz resonance frequency.

At frequencies very much below resonance, the first term on the left-hand side is negligible so that the monopole strength is then

$$\frac{A}{\omega_0^2 L} \frac{\partial^2 p_r'}{\partial t^2} \quad \text{or} \quad \frac{V}{c^2} \frac{\partial^2 p_r'}{\partial t^2}.$$

Then the sound pressure $p(\underline{x}, t)$ radiated to distance $|\underline{x}|$ from the vessel is:

$$p(\underline{x}, t) = \frac{V}{4\pi c^2 |\underline{x}|} \frac{\partial^2}{\partial t^2} p_r' \left(t - \frac{|\underline{x}|}{c_0} \right) \quad \dots (9)$$

The frequency of the aerodynamic pressure p_t is set by the Strouhal number so that;

$$\left| \frac{\partial^2 p'_R}{\partial t^2} \right| \sim \left(\frac{U}{\ell} \right)^2 \left| p'_R \right| \quad \dots (10)$$

and since p'_R increases with the square of velocity, the radiated sound will increase in intensity (p^2) in proportion to the eighth power of velocity. Evidently the containment of aerodynamic sources within a small vessel cannot materially affect the velocity dependance of their radiated sound so long as their frequency content is below the natural resonance frequency of the vessel.

The second term on the left-hand side of equation (8) is negligible at frequencies much above ω_0 . Then the monopole strength is simply

$\frac{A}{L} p'_R$, and the sound field radiated outside V is:

$$p(\underline{x}, t) = \frac{A}{4\pi L|\underline{x}|} p'_R \left(t - \frac{|\underline{x}|}{c_0} \right) \quad \dots (11)$$

The intensity of this high frequency sound scales on the fourth power of velocity. The sound pressure level is in fact independent of the acoustic velocity, so that at low Mach number the containment of high frequency aerodynamic sources within the vessel vastly improves their radiation efficiency.

Resonant Behaviour

According to the foregoing linear theory the response and radiation are unbounded at the resonance frequency. An upper bound can be placed on the radiation by equating the available energy in the flow at this frequency to the sound energy. The energy available in the unsteady flow will scale on the mean kinetic energy, so that the maximum possible radiation power at the resonance condition is proportional to:

$$\bar{\rho} U^3, \quad \dots (12)$$

so that the radiated sound pressure has amplitude scaling on:

$$\bar{\rho} U^2 \left(\frac{c_0}{U} \right)^{1/2} \frac{\sqrt{A}}{|\underline{x}|} \quad \dots (13)$$

The monopole strength thus has a maximum amplitude proportional to $\bar{\rho} U^2 \left(\frac{c_0}{U} A \right)^{1/2}$.

Equation (8) shows that the monopole amplitude at frequency ω is:

$$\frac{\frac{A}{L} \omega^2 p'_r}{(\omega_0^2 - \omega^2)} \dots (14)$$

which approximates $\frac{A}{L} \frac{\omega_0}{2\Delta\omega} p'_r$ at frequency $\omega_0 + \Delta\omega$. The bandwidth of the resonance can be estimated by determining the value of ω for which the source is 3 db down on its resonance value.

$$\frac{A}{L} \frac{\omega_0}{2\Delta\omega} p'_r = \frac{1}{2} \bar{p} U^3 \left(\frac{c_0}{U} \frac{A}{L} \right)^{1/3} \dots (15)$$

$$\frac{\Delta\omega}{\omega_0} \approx \left(\frac{c_0}{U} \frac{L^3}{A} \right)^{1/3} \dots (16)$$

This bandwidth can be rather large at low Mach number so that the resonance peak may be quite broad and no discreet frequency sound could be produced. This resonant response broad band noise would scale with the cube of characteristic speed, according to (13).

Evidently aerodynamic sources radiate sound more efficiently when they are confined in a vessel whose natural Helmholtz resonance frequency is smaller than the Strouhal frequency. The main response is likely to be at resonance where the sound scales on characteristic flow velocity to the third power. The resonance bandwidth could however be very broad at low Mach number. At higher frequencies the radiated sound scales on the fourth power of velocity.

Sources with frequency below the resonance frequency radiate ineffectively with an efficiency depending on velocity in precisely the same way as in unbounded space. Low frequency sound therefore scales on the eighth power of velocity.

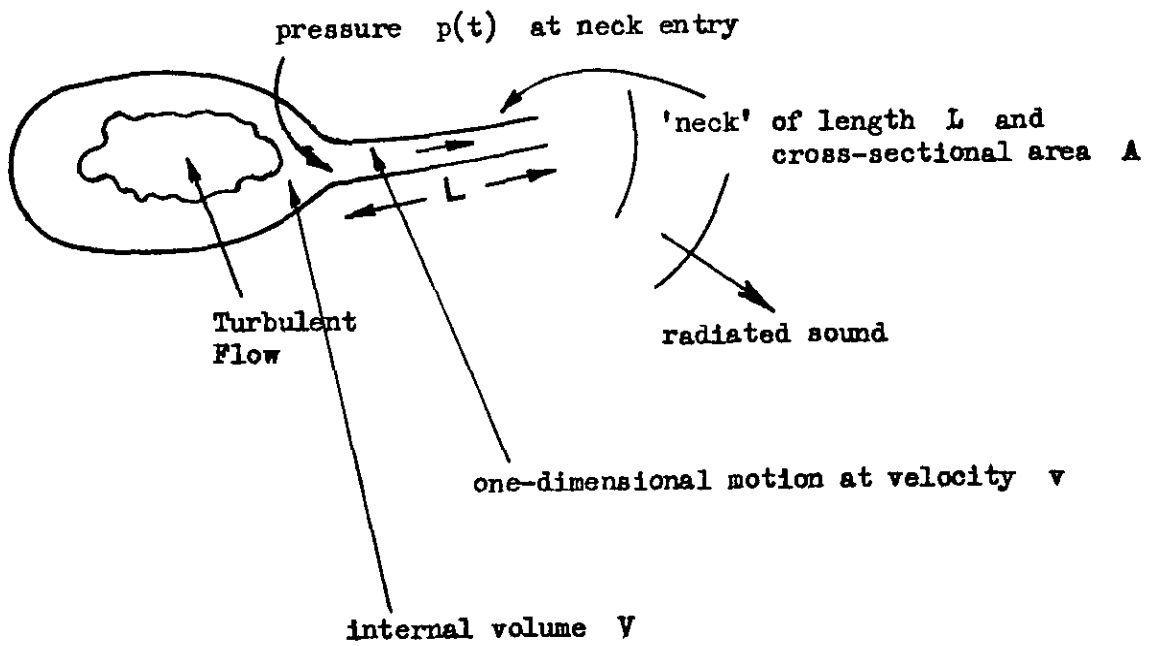


Fig. 1 Illustration of the model problem of sound generation by unsteady flow contained in a Helmholtz resonator

Chapter 2

Transmission of Low Frequency Jet Pipe Sound through a Nozzle Flow

by

John E. Ffowcs Williams,
Department of Mathematics,
Imperial College, London

The model problem is illustrated in Fig. 1. The basic flow is a subsonic jet of velocity V_2 formed by expanding a hot jet pipe flow of mean velocity V_1 and static pressure p_1 in a jet pipe of cross-sectional area A_1 through a nozzle down to the ambient pressure p_0 . The jet flows in the direction $+x$. Superimposed on this basic flow is a low frequency sound wave of pressure p^+ incident from $x < 0$. The meaning of low frequency in this context is that the nozzle scale is much smaller than the wavelength in both the jet stream and the environment. The time dependence is taken as $e^{-i\omega t}$ throughout. The problem is to determine the unsteady conditions at the nozzle exit and the sound field radiated to the static homogeneous environment exterior to the jet.

The incident pressure wave p^+ will be reflected (with reflection coefficient R) at the nozzle as an upstream wave of pressure $p^- = Rp^+$. The perturbation pressure at the entry to the nozzle, station (1), will therefore be the superposition of these waves.

$$p_1^i(t) = (p^+ + p^-) e^{-i\omega t} = (1 + R) p^+ e^{-i\omega t}. \quad \dots (1)$$

The unsteady velocity u' , measured in the $+x$ direction, is therefore:

$$u_1^i(t) = (p^+ - p^-) \frac{e^{-i\omega t}}{\rho_1 c_1} = (1 - R) \frac{p^+}{\rho_1 c_1} e^{-i\omega t} \quad \dots (2)$$

The dependence of p_1^i on u_1^i can be found by considering the pressure gradient required to accelerate the fluid on the jet axis through the nozzle.

$$\frac{1}{\rho} \frac{\partial p}{\partial x} = - \frac{Du}{Dt} = \frac{\partial}{\partial x} \int \frac{dp}{\rho} \quad \dots (3)$$

We assume adiabatic motion with γ equal to the ratio of specific heats.

$$\frac{\gamma}{\gamma - 1} \frac{\partial}{\partial x} \left(\frac{p}{\rho} \right) = - \frac{\partial u}{\partial t} - \frac{\partial}{\partial x} \frac{1}{2} u^2 \quad \dots (4)$$

In the nozzle region, provided the scale L is smaller than the acoustic wavelength, the dependence of u on axial position x is the same as it is in purely steady flow at velocity V . Therefore:

$$u(x,t) = u_1(t) \frac{V(x)}{V_1} \quad \dots (5)$$

Equation (4) can then be integrated on the jet axis over the 'nozzle flow' region between stations 1 and 2.

$$\frac{\gamma}{\gamma - 1} \left(\frac{p_2}{\rho_2} - \frac{p_1}{\rho_1} \right) = - \frac{\partial u_1}{\partial t} \int_1^2 \left(\frac{V}{V_1} \right) (x) dx + \frac{1}{2} u_1^2 - \frac{1}{2} u_2^2 \quad \dots (6)$$

The pressure at station 2 is by definition the constant p_0 , and u_1 is related to u_2 according to equation (5). Equation (6) is therefore an equation relating the pressure and velocity at the nozzle entry so that we can now determine the reflection coefficient for plane waves from equations (1) and (2). The 'nozzle adjustment' length L is defined for convenience as:

$$L = \int_1^2 \frac{2 V(x)}{V_1 + V_2} dx \quad \dots (7)$$

$$\int_1^2 \left(\frac{V}{V_1} \right) (x) dx = \frac{(V_1 + V_2)}{2 V_1} L \quad \dots (8)$$

The unsteady parts of equation (6) are then:

$$\frac{\gamma}{\gamma - 1} \frac{p_1^*}{\rho_1} = \frac{(V_1 + V_2)}{2 V_1} L \frac{\partial u_1^*}{\partial t} + V_1 \left(\frac{V_2^2}{V_1^2} - 1 \right) u_1^* \quad \dots (9)$$

$$\frac{\gamma}{\gamma - 1} (1 + R) \frac{p^*}{\rho_1} = \left[V_1 \left(\frac{V_2^2}{V_1^2} - 1 \right) - i \omega L \frac{(V_1 + V_2)}{2 V_1} \right] (1 - R) \frac{p^*}{\rho_1 c_1} \quad \dots (10)$$

R/

$$R = - \left\{ \frac{1 - \frac{\gamma - 1}{\gamma} \left(M_1^2 \left[\frac{V_2^2}{V_1^2} - 1 \right] - \frac{i\omega L}{c_1} \frac{(V_1 + V_2)}{2V_1} \right)}{1 + \frac{\gamma - 1}{\gamma} \left(M_1^2 \left[\frac{V_2^2}{V_1^2} - 1 \right] - \frac{i\omega L}{c_1} \frac{(V_1 + V_2)}{2V_1} \right)} \right\} \dots (11)$$

where $M_1 = V_1 / c_1$.

$$u_b = \frac{V_2}{V_1} u_1 = \frac{2p^*}{\rho_1 c_1} \frac{V_2}{V_1} \frac{e^{-i\omega t}}{\left\{ 1 + \frac{\gamma - 1}{\gamma} \left[M_1^2 \left(\frac{V_2^2}{V_1^2} - 1 \right) - \frac{i\omega L}{c_1} \frac{(V_1 + V_2)}{2V_1} \right] \right\}} \dots (12)$$

Continuity requires that $\rho_1 A_1 V_1 = \rho_2 A_2 V_2$, so that,

$$u_b = \frac{2p^*}{\rho_2 c_1} \frac{A_1}{A_2} \frac{e^{-i\omega t}}{\left\{ 1 + \frac{\gamma - 1}{\gamma} \left[M_1^2 \left(\frac{V_2^2}{V_1^2} - 1 \right) - \frac{i\omega L}{c_1} \frac{(V_1 + V_2)}{2V_1} \right] \right\}} \dots (13)$$

The pressure radiated by the unsteady flow can be expressed in terms of the velocity perturbation u_b which induces both a monopole and dipole radiation.

$$p(\underline{x}, t) \sim \frac{A_2}{4\pi|\underline{x}|} \left\{ \frac{\partial}{\partial t} (\rho_2 u_b) + 2 \frac{V_2}{c_0} \cos \theta \frac{\partial}{\partial t} (\rho_2 u_b) \right\}_{t - |\underline{x}|/c_0} \dots (14)$$

where $\theta = 0$ is the jet (x) axis.

$$p(\underline{x}, t) \sim \frac{1}{4\pi|\underline{x}|} \left(1 + 2 \frac{V_2}{c_0} \cos \theta \right) \frac{(-i\omega)}{c_1} \frac{2p^* A_1 e^{-i\omega(t - |\underline{x}|/c_0)}}{\left\{ 1 + \frac{\gamma - 1}{\gamma} \left[M_1^2 \left(\frac{V_2^2}{V_1^2} - 1 \right) - \frac{i\omega L}{c_1} \frac{(V_1 + V_2)}{2V_1} \right] \right\}} \dots (15)$$

$$p(\underline{x}, t) \underset{|\underline{x}| \rightarrow \infty}{\sim} - \frac{i\omega A_1 p^+}{2\pi c_1 |\underline{x}|} \frac{\left\{ 1 + 2 \frac{V_2}{c_0} \cos \theta \right\} e^{-i\omega(t - |\underline{x}|/c_0)}}{\left\{ 1 + \frac{\gamma - 1}{\gamma} \left[M_1^2 \left(\frac{V_2^2}{V_1^2} - 1 \right) - \frac{i\omega L}{c_1} \frac{(V_1 + V_2)}{2V_1} \right] \right\}}$$

... (16)

With no flow and no nozzle this result reproduces the leading terms in

(ωa) of Levine and Schwinger's exact result. The first effect of mean (c)

flow is evidently to increase the field in the direction of flow and reduce that in the upstream direction, the increase being by a factor

$\left(1 + 2 \frac{V_2}{c_0} \cos \theta \right)$ on pressure. The other terms influenced by velocity are

negligible at the low frequencies we are considering when there is no nozzle.

The effect of a nozzle is not very marked unless the contraction ratio is high, much higher than is normal in jet engine configurations. ωL/c₁ is by hypothesis held small so that (V₁ + V₂)/2V₁ must reach a value

of about 10 before the ratio $\frac{\omega L}{c_1} \frac{(V_1 + V_2)}{2V_1}$ becomes important in

equation (16). This implies an area contraction ratio of about 20, which is quite outside the range used in real engines. However, it is not so untypical of model scale situations where laboratory nozzle exit flows are made smooth by rapid expansion of a plenum flow. The effect of the contraction is then very marked in that the transmitted sound scales in direct proportion to the incident field in the jet pipe and not to its rate of change. This is made clear by writing the asymptotic form of (16) when V₂/V₁ is very large, but V₂ not much in excess of c₁.

$$p(\underline{x}, t) \underset{|\underline{x}| \rightarrow \infty}{\sim} \alpha \left(1 + 2 \frac{V_2}{c_0} \cos \theta \right) p^+ \frac{a}{|\underline{x}|} e^{-i\omega(t - |\underline{x}|/c_0)}; 1 \gg \frac{\omega L}{c_1} \gg \frac{2V_1}{V_2}$$

... (17)

where α is a constant of order unity and a is the nozzle exit radius.

Influence of the Nozzle Transmission Properties on the Velocity Dependence of Aerodynamic Sound

Suppose as a first instance that the incident pressure field, p^* , is the large scale near field of aerodynamic quadrupoles, i.e. p^* is the fluctuating pressure level in a turbulent flow, proportional to the unsteady Reynolds stress and scaling with $\rho_1 V_1^2$, the characteristic total head at the entry to the nozzle. For area contraction ratios less than about 20 and supposing the Mach numbers are not large, then the radiated sound is given by equation (16) as:

$$p(\underline{x}, t) \underset{|\underline{x}| \rightarrow \infty}{\sim} \frac{-i \omega \sqrt{A_1}}{2\pi V_1} M_1 \rho_1 V_1^2 \frac{\sqrt{A_1}}{|\underline{x}|} \left(1 + 2 \frac{V_2}{c_0} \cos \theta\right) e^{-i\omega(t - |\underline{x}|/c_0)} \dots (18)$$

The mean square sound pressure generated by turbulent flow at the nozzle entry is then of magnitude:

$$\overline{p^2}(\underline{x}) \underset{|\underline{x}| \rightarrow \infty}{\sim} S^2 M_1^2 \frac{A_1}{4\pi |\underline{x}|^2} \left(1 + 2 \frac{V_2}{c_0} \cos \theta\right)^2 \rho_1^2 V_1^4 ; 1 \gg \frac{\omega L}{c_1} \gg \frac{2V_1}{V_2} \dots (19)$$

The Strouhal number based on nozzle entry conditions

$$S = \frac{\omega \sqrt{A_1}}{V_1} \dots (20)$$

will be a slowly varying function of velocity, so that this radiated sound will increase in proportion to the sixth power of jet velocity.

If on the other hand the nozzle is one of extremely high contraction ratio, equation (17) is relevant and nozzle entry turbulence would then induce a radiated sound of mean square pressure:

$$\overline{p^2}(\underline{x}) \underset{|\underline{x}| \rightarrow \infty}{=} \frac{A_2}{|\underline{x}|^2} \rho_1^2 V_1^4 \left(1 + 2 \frac{V_2}{c_0} \cos \theta\right)^2 ; 1 \gg \frac{\omega L}{c_1} \gg \frac{2V_1}{V_2} \dots (21)$$

Suppose now that the pressure incident on the nozzle from upstream is an aerodynamically generated sound wave. Since $\omega L \ll c_1$, all frequencies are below the pipe 'cut-off' frequency and the sound is then in the form of a one-dimensional travelling wave. Davies and Ffowcs Williams (1968) have shown how the sound generated within a pipe scales on the flow parameters in this situation.

$$p^* \doteq \rho_1 V_1^n M_1^n \dots (22)$$

where $n = 1, 0,$ or -1 for compact aerodynamic quadrupoles, dipoles or monopoles, respectively. When this sound is incident on a nozzle of modest

contraction/

contraction ratio, equation (16) shows how the pressure is made more sensitive to velocity.

$$p(\underline{x}, t) \underset{|\underline{x}| \rightarrow \infty}{\sim} - \frac{iS V_1}{\sqrt{A_1}} \frac{A_1 \rho_1 V_1^2 M_1^n}{2\pi c_1 |\underline{x}|} \left(1 + 2 \frac{V_2}{c_0} \cos \theta\right) e^{-i\omega(t - |\underline{x}|/c_0)} \dots (23)$$

Again the Strouhal number is a slowly varying function of flow conditions so that the aerodynamically generated mean square sound pressure radiated through a nozzle flow typical of operational jet engines is:

$$\overline{p^2}(\underline{x}) \underset{|\underline{x}| \rightarrow \infty}{=} \rho_1^2 V_1^4 M_1^{2n+2} \frac{A_1}{|\underline{x}|^2} \left(1 + 2 \frac{V_2}{c_0} \cos \theta\right)^2 \dots (24)$$

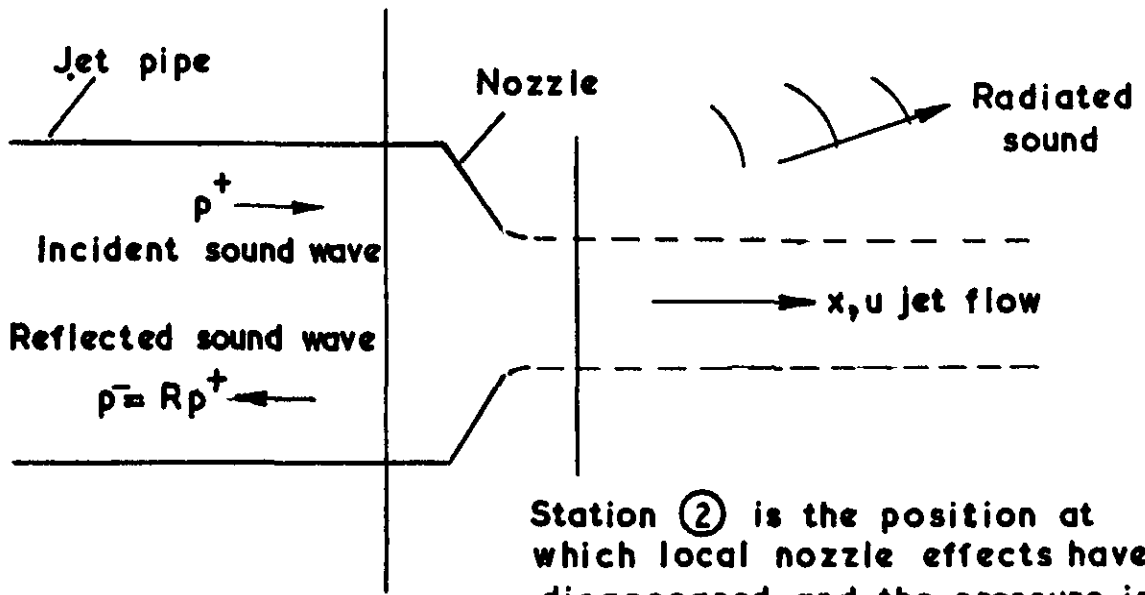
This expression is similar to that describing the radiation of these aerodynamic sources in unbounded free space. The only major effect of their containment within the jet pipe flow terminated by a nozzle is that the directional properties are determined by the jet exit conditions rather than the source orientation. (Though only those multipoles with all axes parallel to the jet axis can radiate at all). The sound field scales on jet pipe conditions upstream of the nozzle. It also scales on the sound speed upstream of the nozzle, and is in this way different from aerodynamic sound in free space which scales on the sound speed of the environment. The difference is a reflection of the fact that in this problem the aerodynamic sources first generate a sound field within the jet pipe and their ability to do this depends on the acoustic speed within the pipe and not on external conditions. The parameter range described by this result is probably typical of all jet engine conditions so that we can conclude that aerodynamic sources contained within the jet but positioned many wavelengths upstream of the nozzle will generate sound depending on jet velocity in precisely the same way as if the sources were in direct communication with the nozzle exterior.

On the other hand if the nozzle contraction ratio is very large then equation (17) is relevant and the sound of contained aerodynamic sources described by equation (22) is heard outside the jet flow with a mean square pressure of magnitude:

$$\overline{p^2}(\underline{x}) \underset{|\underline{x}| \rightarrow \infty}{=} \rho_1^2 V_1^4 M_1^{2n} \frac{A_2}{|\underline{x}|^2} \left(1 + 2 \frac{V_2}{c_0} \cos \theta\right)^2 \dots (25)$$

The velocity dependence is then V_1^6 , V_1^4 and V_1^2 for quadrupoles, dipoles and monopoles respectively.

Station ① immediately prior to position at which pipe flow begins to adjust to the nozzle conditions.



Station ② is the position at which local nozzle effects have disappeared and the pressure is relieved to the constant static pressure p_0 .

Nozzle adjustment length = L

Fig. 1 Diagram illustrating the model problem

Chapter 3

Radiation Properties of the Semi-Infinite Vortex Sheet

by

D. G. Crighton,
Department of Mathematics,
Imperial College, London

ABSTRACT

An exact calculation is given of the acoustic radiation from a time dependent flow coupled to an inhomogeneous solid surface. Specifically, the flow consists of a vortex sheet leaving a semi-infinite plate and undergoing a two-dimensional spatial Kelvin-Helmholtz instability. In the absence of the plate, such an instability mode of the vortex sheet generates no sound. In the presence of a rigid plate, it is found that the intensity-directivity law is

$$I \sim U^4 \sin^2 \theta / 2$$

with θ measured from the downstream direction. If the plate is compliant and fluid loading effects high, the radiation is weaker, with

$$I \sim U^5 \sin^2 \theta .$$

These results agree completely with those predicted from general theories of the scattering of the near-field of point quadrupoles by large wedge-shaped surfaces (Ffowcs Williams and Hall 1970; Crighton and Leppington 1970, 1971). Imposition of the "rectified" Kutta condition of Orszag and Crow (1970) does not modify the sound field. Application of the "full" Kutta condition, that the sheet leaves the plate at zero gradient, results in an enormous increase in the radiation, with

$$I \sim U^2 \operatorname{cosec}^2 \theta / 2 .$$

1. Introduction

An area of aerodynamic noise theory in which significant advances have recently been made is that of the interaction of unsteady flows with solid surfaces. The possibility that the presence of solid surfaces could greatly enhance the radiation from a contiguous turbulent flow was first demonstrated by Curle (1955). Subsequently, this possibility became a matter of some controversy (Meecham (1963), Powell (1963), Ffowcs Williams (1963)), which the papers of Ffowcs Williams (1965), Ffowcs Williams and Hall (1970), Davies (1970) and Crighton and Leppington (1970, 1971) have attempted to resolve. These papers, and others referenced in them, while providing a basic understanding of most effects likely to occur in practice, involve a considerable, and perhaps unjustified, extrapolation from Lighthill's (1952) original theory of aerodynamic sound in the absence of surfaces. The view is taken that the flow is acoustically equivalent to a volume distribution of quadrupoles, and that details of the flow serve merely to determine the strength and frequency content of that distribution. Thus the problem of flow noise in the presence of surfaces is reduced to one of classical diffraction theory - essentially that of finding the solution to the linearised wave equation with a point quadrupole inhomogeneity, subject to the boundary conditions demanded by the surface under discussion. The hydrodynamic aspect of the problem is completely contained in the strength and frequency parameters of the quadrupole inhomogeneity. Such a de-coupling of hydrodynamics and acoustics has its difficulties even in the case of free turbulence, and clearly requires adequate justification, since it is the crux of the surface scattering theories cited above.

In the case of free turbulence, the appropriate justification has been given by Crow (1970), who also gives a penetrating discussion of the very severe limitations on the quadrupole model. An extension of his methods and results to the case of a general flow in the presence of any surface likely to be of practical significance appears to set a formidable problem. Accordingly, expediency seems to require the necessary justification for scattering theories to come from a comparison of their predictions with exact solutions for particular flows. For example, the low Mach number radiation from a line vortex spinning about a circular cylinder, whose axis is parallel with that of the vortex, is capable of calculation (Heckl, 1970), with results which agree with those of Curle (1955) and Crighton and Leppington (1971). The cylinder scatters a dipole field, if its radius is less than the relevant acoustic wavelength, with intensity increasing as the fifth power of a typical flow speed U . In contrast, a spinning vortex pair in free space radiates a quadrupole field with intensity varying as U^7 (Obermeier, 1967). Examples of greater practical significance are not easily found, and the flow discussed in the sequel seems to provide the first case of a flow which is in some sense extended in space, and coupled to a non-trivial surface of practical interest. (The flows discussed by Amiet and Sears (1970) are of a rather different kind, involving motions essentially driven by the prescribed motion of a surface; what we require are flows coupled to surfaces which are passive, except for their rôle as scattering centres).

The flow whose acoustic properties form the subject of this paper was first examined by Orszag and Crow (1970), in the context of hydrodynamic stability theory. Plane parallel flow on one side of a semi-infinite plate generates a vortex sheet downstream of the trailing edge,

which/

which may develop a time-harmonic spatially growing instability. Orszag and Crow determine the correction caused by the presence of the plate to the Kelvin-Helmholtz instability eigenfunctions of the doubly infinite vortex sheet. Their conclusions are essentially that the correction is negligible at distances greater than a hydrodynamic wavelength from the edge. Such an effect is of no great significance for stability theory, but the flow is of the greatest interest in the context of aerodynamic noise theory. We shall see that the flow is an extremely efficient radiator of sound - entirely because of the small correction required by the presence of the plate, for at subsonic flow speeds a Helmholtz instability on a doubly infinite vortex sheet radiates no sound field at all. One very interesting aspect of the work of Orszag and Crow involves the application of two possible Kutta conditions, both of which have important consequences in the acoustic problem. The appropriate compressible generalisations of the functions used by Orszag and Crow to enforce Kutta conditions are found in Section 4. We start, however, by considering the Orszag-Crow problem for a compressible fluid at low Mach numbers. The first section consists merely of a recapitulation of the derivation of the correction field due to the presence of a rigid plate, this being needed primarily because it is not at all obvious that a knowledge of surface pressure fields according to incompressible flow theory is adequate for an evaluation of the distant sound field when the surface concerned is large compared with an acoustic wavelength. Subsequent sections then discuss the effects of substantial compliance of the plate, the imposition of Kutta conditions, and the generalisation of Sommerfeld's classical half-plane diffraction problem to incorporate the effect of the vortex sheet. The paper ends with a discussion of the relevance of the results to current problems in jet noise prediction. It is suggested that the interaction of shear layer instability with a large solid surface may be the mechanism responsible for the so-called "excess noise" phenomenon.

2. Vortex Sheet Leaving a Rigid Plate

We consider two-dimensional motion in the (x,y) plane (Fig. 1). A semi-infinite rigid plate lies in $y = 0$, $x < 0$. In the unperturbed state, the fluid in $y > 0$ is at rest, while that in $y < 0$ streams uniformly with velocity $(U,0)$. The fluid density ρ_0 and the sound speed a_0 are the same in both regions, and we assume that $M = U/a_0 < 1$.

We seek the eigenmodes of the coupled fluid-plate system, subject to linearised theory and to the assumption that a steady state exists in which all fluctuating quantities have the time dependence $\exp(-i\omega t)$, $\omega > 0$. This assumption requires that solutions exponentially large as $x \rightarrow +\infty$ must be admitted. Orszag and Crow (1970) remark that, in an elliptic problem of the present kind, this constitutes a real logical difficulty, in that the actual behaviour as $x \rightarrow +\infty$ must be dominated by non-linear and viscous effects, and that such deviation from the linear solution might have a large effect throughout the whole flow. The alternative involves a study of the initial value problem for a temporal instability. This, however, merely transfers the difficulty to another stage, as can be seen from the work of Howe (1970) on the doubly-infinite vortex sheet. There, the increase of growth rate with frequency leads to a divergent integral for the response to impulsive excitation; Howe arbitrarily truncates the integrand beyond finite limits, but the solution is then highly sensitive to the form of cut-off adopted. And in any case, the impulsively

generated/

generated flow bears very little relation to flows of practical interest, which are almost invariably at least statistically steady in time, so that the spatial instability problem is in fact less open to objection than the initial value problem.

The perturbation potentials satisfy the equations

$$\begin{aligned}
 (\nabla^2 + k_0^2) \phi^{(1)} &= 0, \\
 \left[\nabla^2 - \left(M \frac{\partial}{\partial x} - ik_0 \right)^2 \right] \phi^{(2)} &= 0,
 \end{aligned}
 \tag{2.1}$$

in which $k_0 = \omega/a_0$ is the acoustic wavenumber. In accordance with common practice, it will be convenient to take k_0 as complex, $k_0 = k_1 + ik_2$, with $k_1, k_2 > 0$. An outgoing solution for $\phi^{(1)}$ as $|x| \rightarrow \infty$ is then exponentially damped, $\phi^{(1)} \sim \exp(-k_2 |x|)$, while the behaviour of an outgoing wave $\phi^{(2)}$ is different depending upon the sign of x . As $x \rightarrow +\infty$, $\phi^{(2)} \sim \exp(-k_2 x/(1+M))$, whereas when $x \rightarrow -\infty$, $\phi^{(2)} \sim \exp(-k_2 |x|/(1-M))$.

Kinematic requirements on the vortex sheet $y = \eta(x)\exp(-i\omega t)$ are expressed by

$$\begin{aligned}
 \frac{\partial \eta}{\partial t} &= \frac{\partial \phi^{(1)}}{\partial y}, \\
 \frac{\partial \eta}{\partial t} + U \frac{\partial \eta}{\partial x} &= \frac{\partial \phi^{(2)}}{\partial y}
 \end{aligned}
 \tag{2.2}$$

for $y = 0$, $x > 0$, and the dynamic condition, that the vortex sheet cannot withstand a pressure jump across it, requires that

$$\frac{\partial \phi^{(2)}}{\partial t} + U \frac{\partial \phi^{(2)}}{\partial x} = \frac{\partial \phi^{(1)}}{\partial t}
 \tag{2.3}$$

on $y = 0$, $x > 0$. The conditions on the rigid plate are simply that

$$\frac{\partial \phi^{(1)}}{\partial y} = \frac{\partial \phi^{(2)}}{\partial y} = 0, \quad y = 0, \quad x < 0.
 \tag{2.4}$$

We follow Orszag and Crow (1970) in isolating a contribution to the field consisting of a Helmholtz instability, growing as $x \rightarrow +\infty$ as if on a doubly-infinite vortex sheet. Assuming a space dependence

exp/

$\exp(-i\alpha x)$, the Helmholtz instability is defined by

$$\begin{aligned}\phi^{(1)} &= A \exp(-i\alpha x - \gamma_\alpha y) \\ \phi^{(2)} &= B \exp(-i\alpha x + w_\alpha y) \\ \eta &= d \exp(-i\alpha x),\end{aligned}\quad \dots (2.5)$$

where $\gamma_\alpha = (\alpha^2 - k_0^2)^{1/2}$, $\text{Re } \gamma_\alpha > 0$ and $w_\alpha = \{\alpha^2 - (k_0 + \alpha M)^2\}^{1/2}$, $\text{Re } w_\alpha > 0$, in order that the fields be finite for any fixed x as $|y| \rightarrow \infty$. Application of the boundary conditions (2.2) and (2.3) for all x gives

$$\begin{aligned}i\omega D_\alpha d &= -w_\alpha B, \\ i\omega d &= \gamma_\alpha A, \\ D_\alpha B &= A,\end{aligned}\quad \dots (2.6)$$

with $D_\alpha = 1 + \alpha U/\omega = 1 + M\alpha/k_0$, and shows that α is a root of the equation

$$\gamma_\alpha D_\alpha^2 + w_\alpha = 0. \quad \dots (2.7)$$

For the present we are concerned only with $M \ll 1$, in which case (2.3) has two roots,

$$\alpha = -k_H(1 \pm i) + O(M^2 k_H), \quad \dots (2.8)$$

$k_H = \omega/U$ denoting the hydrodynamic wavenumber at frequency ω . We denote the roots (2.8) by $\alpha = \mu, \nu$, these having positive and negative imaginary parts, respectively. Thus the mode $\exp(-i\nu x) \sim \exp(ik_H x - k_H x)$ is evanescent as $x \rightarrow +\infty$, while the mode $\exp(-i\mu x) \sim \exp(ik_H x + k_H x)$

represents a Kelvin-Helmholtz instability growing exponentially in the downstream direction.

The functions in equation (2.5) do not satisfy the boundary conditions (2.4) on the plate. We therefore add correction functions ϕ, ψ and ζ to $\phi^{(1)}, \phi^{(2)}, \eta$, and determine them using the Wiener-Hopf technique. This method serves only to determine a certain class of solutions, as we shall see later. Introduce the full and half range Fourier transforms

$$Z(s) = \int_{-\infty}^{+\infty} \zeta(x) e^{isx} dx ,$$

$$Z_+(s) = \int_0^{+\infty} \zeta(x) e^{isx} dx ,$$

$$Z_-(s) = \int_{-\infty}^0 \zeta(x) e^{isx} dx ,$$

(where we define $\eta(x) = 0$ for $x < 0$), and correspondingly for the transforms $\Phi(s,y)$ of $\phi(x,y)$ and $\Psi(s,y)$ of $\psi(x,y)$. Then the differential equations (2.1) have the solutions

$$\begin{aligned} \Phi(s,y) &= \Phi(s,0) \exp(-\gamma_s y) , \\ \Psi(s,y) &= \Psi(s,0) \exp(+w_s y) , \end{aligned} \quad \dots (2.9)$$

and these imply that

$$\begin{aligned} \Phi'_+(s,0) + \Phi'_-(s,0) &= -\gamma_s \left[\Phi_+(s,0) + \Phi_-(s,0) \right] , \\ \Psi'_+(s,0) + \Psi'_-(s,0) &= +w_s \left[\Psi_+(s,0) + \Psi_-(s,0) \right] , \end{aligned} \quad \dots (2.10)$$

the prime indicating differentiation with respect to y . Transformation of the boundary conditions (2.2) and (2.3) gives the relations among plus functions

$$\begin{aligned} -i\omega Z_+(s) &= \Phi'_+(s,0) , \\ -i\omega D_s Z_+(s) &= \Psi'_+(s,0) + U \zeta_0 , \\ -i\omega D_s \Psi_+(s,0) &= -i\omega \Phi_+(s,0) + U \psi_0 \end{aligned} \quad \dots (2.11)$$

where $\zeta_0 = \zeta(x=0)$, $\psi_0 = \psi(x=y=0)$, while the conditions (2.4) on the plate give

$Z_- /$

$$\begin{aligned}
 Z_-(s) &= \frac{id}{s - \mu} , \\
 \phi'_-(s,0) &= -\frac{iy_\mu A}{s - \mu} , \quad \dots (2.12) \\
 \psi'_-(s,0) &= \frac{iw_\mu B}{s - \mu} .
 \end{aligned}$$

Elimination of all plus functions except $Z_+(s)$ from (2.10), (2.11) and (2.12) then leads to the following standard⁺ form of Wiener-Hopf equation (the direct analogue, for compressible flow, of equation (3.19) of Orszag and Crow (1970)),

$$-i\omega Z_+(s) = K(s) \left[D_s \psi_-(s,0) - \phi_-(s,0) + \frac{iU\psi_0}{\omega} \right] + \frac{iy_\mu A}{s - \mu} , \quad \dots (2.13)$$

in which the kernel $K(s)$ is given by

$$K(s) = \frac{w_s \gamma_s}{(\gamma_s D_s^2 + w_s)} = \frac{w_s \gamma_s}{M(s)} , \quad \dots (2.14)$$

$$M(s) = (s^2 - k_0^2)^{1/2} \left(1 + \frac{Ms}{k_0} \right)^2 + \left\{ s^2 - (k_0 + sM)^2 \right\}^{1/2} .$$

The usual considerations (Noble 1958, p.53) indicate that for $M < 1$ the domain of regularity in which all functions in (2.13) are analytic is the strip

$$\mathcal{D} : -\frac{k_s}{1+M} < \text{Im } s < +k_s ,$$

and therefore that the correction functions to be obtained from (2.13) vanish as $|x| \rightarrow \infty$ at least as fast as an outgoing diffracted wave field of the kind discussed following equation (2.1).

The kernel $K(s)$ can be factorised in the form

$$K(s) = K_+(s) K_-(s)$$

where the factors are analytic and non-zero in $\text{Im } s > -k_s/(1+M)$ and $\text{Im } s < +k_s$ respectively, and where $K_+(s)$ are each $O(s^{-1/2})$ as $|s| \rightarrow \infty$ in appropriate upper and lower half-planes. Consequently we can carry out the usual rearrangements to get

$$\begin{aligned}
 & - \frac{i\omega Z_+(s)}{K_+(s)} - \frac{iy_\mu A}{(s-\mu)} \left(\frac{1}{K_+(s)} - \frac{1}{K_+(\mu)} \right) \\
 & = K_-(s) \left[D_s \Psi_-(s,0) - \Phi_-(s,0) + \frac{iU\psi_0}{\omega} \right] \\
 & \quad + \frac{iy_\mu A}{K_+(\mu)(s-\mu)},
 \end{aligned}$$

so that each side must be the representation in the appropriate half-plane of the same entire function $E(s)$. But as $x \rightarrow 0+$, $\zeta(x)$ is finite, if the vortex sheet is to remain attached to the plate, while the potentials ϕ, ψ can be required to be finite near the trailing edge. Therefore $Z_+(s)$, $\Phi_-(s,0)$ and $\Psi_-(s,0)$ are each $O(s^{-1})$ at infinity in their respective domains of analyticity, and $E(s)$ then vanishes at infinity throughout the complex s -plane at least as fast as $s^{-1/2}$. By Liouville's theorem, $E(s)$ must vanish identically, and we thus obtain the solutions

$$\begin{aligned}
 i\omega Z_+(s) &= - \frac{iy_\mu A}{s-\mu} \left(1 - \frac{K_+(s)}{K_+(\mu)} \right), \\
 \Phi(s,0) &= \frac{iy_\mu A}{\gamma_s(s-\mu)} \frac{K_+(s)}{K_+(\mu)}, \\
 \Psi(s,0) &= - \frac{iy_\mu A}{\omega_s(s-\mu)} \frac{D_s K_+(s)}{K_+(\mu)}.
 \end{aligned} \tag{2.15}$$

Note that no attempt has been made yet to enforce any type of Kutta condition at the trailing edge. Thus from (2.15) it can be shown that $\zeta = O(x^{1/2})$, $\phi = O(|x|^{3/2})$ and $\psi = O(|x|^{1/2})$ near $x = 0$, so that the perturbation velocities in $y < 0$ and the gradient of the vortex sheet both become infinite like $x^{-1/2}$ at the edge.

The fluctuation quantities in real space are found by Fourier inversion. We are interested here in the radiated field in the stagnant fluid $y > 0$, for which

$$\phi(x,y) = \frac{1}{2\pi} \int_{-\infty+i\epsilon}^{+\infty+i\epsilon} \Phi(s,0) e^{-isx-\gamma_s y} ds$$

where

$$- \frac{k_s}{1+M} < \epsilon < + k_s.$$

Evaluation of such integrals is a standard procedure of diffraction theory (e.g. Noble 1958, p.31), and we merely state that the pole of $\Phi(s,0)$ at $s = \mu$ can be shown to play no part in a straightforward steepest descent calculation which leads to

$$\phi(r,\theta) \sim \left(\frac{k_0}{2\pi r}\right)^{1/2} e^{ik_0 r - i\pi/4} \frac{\gamma_\mu A}{k_0(\mu + k_0 \cos \theta)} \frac{K_+(-k_0 \cos \theta)}{K_+(\mu)}, \quad \dots (2.16)$$

uniformly in θ (where $x = r \cos \theta$, $y = r \sin \theta$, $0 < \theta < \pi$) provided $k_0 r \gg 1$ and $M \ll 1$.

A general decomposition of $K(s)$ for arbitrary M is made exceedingly difficult by the presence of four branch points. Here, fortunately, we are concerned only with the case $M \ll 1$, for which the kernel $K(s)$ may be uniformly approximated by

$$K(s) \sim \gamma_s \left[\left(1 + \frac{Ms}{k_0}\right)^2 + 1 \right]^{-1/2},$$

with a relative error $O(M)$, uniformly in s . The factorisation is then immediate; we have

$$\begin{aligned} K_+(s) &= \left(\frac{k_0}{M}\right) \frac{(s + k_0)^{1/2}}{(s - \nu)}, \\ K_-(s) &= \left(\frac{k_0}{M}\right) \frac{(s - k_0)^{1/2}}{(s - \mu)}, \end{aligned} \quad \dots (2.17)$$

where the wavenumbers μ, ν are defined following (2.8) and the factors are analytic and non-zero in the appropriate upper and lower half-planes.

We now insert the expressions of (2.17) into (2.16) to find

$$\phi(r,\theta) \sim \left(\frac{2^{1/2}}{\pi k_H r}\right)^{1/2} e^{ik_0 r - 3\pi i/8} A \sin \theta/2, \quad \dots (2.18)$$

for $M \ll 1$. To compare this result with others of aerodynamic noise theory, we define a hydrodynamic length scale ℓ by $\ell = U/\omega = k_H^{-1}$, and regard

the basic incompressible flow as defined by the length and velocity scales ℓ, U alone, so that $A \sim U\ell$. The radiated density fluctuation then follows directly from (2.18) as

$$\rho' \sim \rho_0 \left(\frac{\ell}{r}\right)^{1/2} M^2 \sin \theta/2. \quad \dots (2.19)$$

and/

and the intensity-directivity law is

$$I \sim U^4 \sin^2 \theta / 2 . \quad \dots (2.20)$$

Now the sound field resulting from the interaction of a general three-dimensional flow field with a semi-infinite rigid plate has been examined by Ffowcs Williams and Hall (1970), in the context of Lighthill's (1952) equivalent quadrupole model, with the conclusion that $I \sim U^5 \sin^2 \theta / 2$. The analogous result for a two-dimensional flow field, although not given by Ffowcs Williams and Hall, is precisely (2.20). This can be seen from the systematic method proposed by Crighton and Leppington (1970, 1971) for attacking two and three-dimensional scattering problems, involving the use of the Reciprocal Theorem and the solution of a two-dimensional diffraction problem. The scattering efficiency of a quadrupole/plate system is basically the same whether line or point quadrupoles are considered. However, the free-field intensity radiated by a two-dimensional quadrupole varies as U^7 instead of the familiar U^8 in three dimensions (Ffowcs Williams, 1969), and therefore the U^5 of Ffowcs Williams and Hall is reduced in our problem to U^4 , all other factors remaining essentially unchanged.

The work of this section thus bears out exactly the predictions of the general theory of quadrupole near-field scattering by a rigid half-plane. The velocity index and directivity appearing in (2.20) are both highly significant for certain difficulties in the application of aerodynamic noise theory to the prediction of the noise levels of current jet engines, and a discussion of the importance of the law (2.20) follows in Section 6.

3. Vortex Sheet Leaving a Compliant Plate

We now relax the condition that the plate be rigid, and consider the case of a "locally reacting" compliant plate endowed with mass m per unit area and negligible bending stiffness. For $x < 0$, $\eta(x)$ will denote the plate deflexion. Then the kinematic conditions (2.2) are to be enforced for all values of x . For $y = 0$ and $x > 0$ we still have the condition (2.3), that the vortex sheet cannot withstand a pressure jump, while for $y = 0$, $x < 0$ the pressure jump across the plate must balance the rate of change of surface momentum, so that

$$\rho_0 \frac{\partial \phi^{(1)}}{\partial t}(x, 0) - \rho_0 \left(\frac{\partial}{\partial t} + U \frac{\partial}{\partial x} \right) \phi^{(2)}(x, 0) = m \frac{\partial^2 \eta}{\partial t^2} . \quad \dots (3.1)$$

Writing the potentials $\phi^{(1)}$, $\phi^{(2)}$ and the deflexion η as the sum of Helmholtz terms (equation (2.5)) in the absence of any surface plus corrections ϕ , ψ , ζ respectively, it is a straightforward matter to derive the Wiener-Hopf equation

$$Z_+(s) = \frac{i \rho_0}{m \omega} L(s) F_-(s) - \frac{id}{s - \mu} , \quad \dots (3.2)$$

in which $F_-(s) = D_B \Psi_-(s,0) - \Phi_-(s,0) + \frac{iU\psi_0}{\omega}$,

$$L(s) = 1 + \frac{m w_B \gamma_B}{\rho_0} \left(w_B + \gamma_B D_B^2 \right)^{-1} \quad \dots (3.3)$$

In the limit of infinite surface mass, the equation (2.13) is, of course, immediately recovered.

Proceeding as in the previous section, a formal solution to (3.2) gives the expression

$$Z(s) = \frac{id \{L(s) - 1\}}{(s - \mu) L_-(s) L_+(\mu)} \quad \dots (3.4)$$

for the full-range transform of the correction to the deflexion of the vortex sheet/plate system, and the far-field radiation in the stagnant fluid is given by

$$\phi(r, \theta) \sim \left(\frac{1}{2\pi k_0 r} \right)^{1/2} e^{ik_0 r - i\pi/4} \frac{\gamma_\mu \Delta \{L(-k \cos \theta) - 1\}}{(\mu + k \cos \theta) L_+(\mu) L_-(-k \cos \theta)} \quad \dots (3.5)$$

The case of low fluid loading, $mk_0/\rho_0 \gg 1$, merely involves perturbations away from the results of Section 2, and is of no further interest. In the high fluid loading limit, $mk_0/\rho_0 \ll 1$, it is evident that

$$L(s) = 1 + O\left(\frac{mk_0}{\rho_0}\right)$$

uniformly in s , provided also that $M \ll 1$. Because of the presence of the factor $L(-k \cos \theta) - 1$ in (3.5) it is therefore sufficient to take $L_+(\mu) = L_-(-k \cos \theta) = 1$, and then we have

$$\phi(r, \theta) \sim \left(\frac{1}{2\pi k_0 r} \right)^{1/2} e^{ik_0 r + i\pi/4} \Delta \left(\frac{mk_0}{2\rho_0} \right) \sin \theta. \quad \dots (3.6)$$

Introducing the length $\ell = U/\omega$ as before, the intensity-directivity law replacing (2.20) is

$$I \sim \frac{U^2 \sin^2 \theta}{\epsilon^2}, \quad \dots (3.7)$$

where the fluid loading parameter ϵ is defined by

$$\epsilon = \frac{2\rho_0 \ell}{m}$$

Now/

Now the quadrupole scattering problem for a compliant plate has been examined by Crighton and Leppington (1970), with the conclusion that $I \sim U^6 \epsilon^{-1} \sin^2 \theta R^{-3}$ for a three-dimensional point quadrupole distant R from the plate edge. For a two-dimensional quadrupole, U^6 is reduced to U^5 as noted earlier. Thus (3.7) reproduces the predictions of point quadrupole scattering theory exactly, except in the dependence upon ϵ . The failure in this respect is not surprising, since a volume integration of the factor R^{-3} over all quadrupoles lying within a certain region of the edge is required for the total intensity of an extended flow. Though difficult to define precisely, in view of the complexity of certain functions arising in the scattering problem, the integration limits are certainly dependent upon ϵ , and it is this fact which causes the ϵ -dependence of (3.7) to differ from that of an isolated quadrupole.

By comparing (3.7) with (2.20), we conclude that the effect of substantial surface compliance is to reduce the radiated intensity by one power of Mach number, and to cause a shift of the directional maximum of the intensity from the upstream direction $\theta = \pi$ to the broadside direction $\theta = \pi/2$. A still more drastic change in the radiation properties of the flow results from the application of a Kutta condition at the trailing edge, and the manner in which this is accomplished is described in the next section.

4. Imposition of Kutta Conditions

In their discussion of the incompressible vortex sheet flow leaving a rigid plate, Orszag and Crow (1970) distinguish between two possible Kutta conditions which might appropriately be enforced, depending upon circumstances in the unperturbed flow, and show how these may be incorporated into the analysis. The condition which they consider most apposite to the present problem involving only one mean (zero-order) velocity field is called a "rectified" Kutta condition, and requires the vortex sheet at no time to have positive gradient as it leaves the trailing edge of the plate. For suppose that the sheet could leave the plate with positive gradient. Then the basic flow in region 2 would be required to negotiate a turn round an angle greater than π . In a real fluid, any such attempt would result in the shedding of vorticity of such a sign as to reduce the vortex sheet gradient at the trailing edge. This is the first step in establishing a first order mean circulation change across the plate, and it is repeated with cumulative effect in the corresponding parts of all subsequent cycles of the system. In the other parts of the cycle - i.e. when the sheet bends downwards into the mainstream, there is no zero-order flow above the sheet able to convect any detached vorticity away from the edge. Thus a continually increasing distribution of vorticity of one sign is formed downstream of the trailing edge, until a steady state is reached in which the sheet never leaves the plate upwards into the stagnant fluid, and no more excess vorticity is shed.

The rectified Kutta condition is imposed by adding to the oscillatory displacement $\eta(x)e^{i\omega t}$ determined in Section 2 a time-independent parabolic displacement $\eta(x,t) = -a(2x)^{1/2}$. Corresponding potentials satisfying $\nabla^2 \phi^{(1)} = 0$ and $(\nabla^2 - M^2 \partial^2 / \partial x^2) \phi^{(2)} = 0$, together with all the boundary conditions (2.2, 2.3 and 2.4) on the plate and on the vortex sheet, are $\phi^{(1)} = 0$ and $\phi^{(2)} = Ua \{ [x^2 + (1-M^2)y^2]^{1/2} - x \}^{1/2}$, the latter being simply the slender-body version of potential flow past a parabolic cylinder. Suitable choice of a , in fact

$$a = \frac{2A}{U} \left\{ \frac{2(i+1)k_H}{\pi} \right\}^{1/2},$$

ensures that the sheet always leaves the plate downwards into the main flow.

This step does not remove the apparently singular nature of the derivatives of $\phi^{(2)}$ at the plate edge. In fact, as noted before, one can show from (2.15) that $\eta \sim x^{1/2}$, $\phi^{(2)} \sim x^{1/2}$ on $y = 0$, $x > 0$, but that the velocity components in the stagnant fluid remain finite. More generally one can show (Orszag and Crow, (1970) that these values of η , $\phi^{(2)}$ correspond exactly to the slender-body approximation to steady flow past a certain parabola, the time dependence of the problem vanishing at distances less than about k_H^{-1} from the edge. But that information allows us to disregard the singularities of $\phi^{(2)}$ as an irrelevancy which has been introduced by the slender-body linearisation. The full potential for the flow past a parabola has no singularity at the vertex, but linearisation transfers a singularity from the focus to the vertex.

Further details are given by Orszag and Crow. The point of importance here is that the rectified Kutta condition can be met by the superposition of a time-independent flow field onto the results of Section 2, and involves no change whatsoever to those results on the radiation from the flow.

The other possible Kutta condition, the "full" condition, requires the sheet to leave the plate with zero gradient at all times. This condition clearly has more relevance to problems in which there is a zero-order mean flow on both sides of the plate (indeed, Orszag and Crow (1970) regard the application of the full condition to the present problem as indefensible), but even so, cannot be expected to apply unless frequencies are low enough to permit the necessary vorticity to be shed and to react back on the flow within each cycle. Nonetheless, application of the full condition has such dramatic consequences for the sound field that a brief outline of the analysis is worthwhile even if it is felt that the full condition will not often be met in practice.

In the case of incompressible flow, Orszag and Crow (1970) show how the full Kutta condition may be imposed by separating terms $\pm Q [(x^2 + y^2)^{1/2} - x]^{1/2} \exp(-i\omega t)$ from the potentials $\phi^{(1)}$, $\phi^{(2)}$, (in addition to the Helmholtz modes of the doubly infinite vortex sheet) and requiring the correction potentials ϕ, ψ to account for the failure of these terms to satisfy conditions across the vortex sheet as well as for the misbehaviour of the Helmholtz modes on the plate. The constant Q can be found in terms of the amplitude A of the Helmholtz mode in such a way as to ensure that $\eta(x) = O(x^{3/2})$ as $x \rightarrow 0+$, in accordance with the full Kutta condition.

Consider first the potential in the stagnant fluid. The generalisation of the Orszag and Crow potential $[(x^2 + y^2)^{1/2} - x]^{1/2}$ to a compressible fluid must satisfy $(\nabla^2 + k_0^2) \phi^{(1)} = 0$, represent an outgoing wave field everywhere at infinity, and reduce to $[(x^2 + y^2)^{1/2} - x]^{1/2}$ as $k_0 r \rightarrow 0$.

The appropriate potential is to be found from Lamb's (1907) work on scattering by a parabolic cylinder.

Defining

$$G(v) = \int_v^{\infty} \exp(2it^2) dt,$$

the function

$$\phi^{(1)} = \exp(ik_0 x) G \left\{ (k_0 r)^{1/2} \sin \frac{\theta}{2} \right\} \quad \dots (4.1)$$

satisfies the Helmholtz equation, has a variable part $-(k_0 r)^{1/2} \sin \theta/2$ as $k_0 r \rightarrow 0$, behaves like $\exp(ik_0 x)$ on $\theta = 0$ and like

$$-\frac{\exp(ik_0 r)}{2i(k_0 r)^{1/2} \sin \theta/2}, \quad (k_0 r \rightarrow \infty, \theta = 0) \quad \dots (4.2)$$

and thus satisfies all the required conditions.

For the potential in region 2 we have to satisfy $[\nabla^2 - (M \partial/\partial x - ik_0)^2] \phi^{(2)} = 0$ with a similar kind of function. A simple transformation, amounting to a Doppler shift of the wavenumber and a Prandtl-Glauert stretching of the y-coordinate, shows that if

$$\phi^{(1)} = \exp(ik_0 x) G \left\{ (k_0 r)^{1/2} \sin \frac{\theta}{2} \right\} = \exp(ik_0 x) V(x, y; k_0)$$

then the corresponding function for region 2 is

$$\phi^{(2)} = \exp\left(\frac{ik_0 x}{1+M}\right) V\left(x, y \sqrt{1-M^2}; \frac{k_0}{1-M^2}\right).$$

Thus we define new correction functions ϕ, ψ, ζ by

$$\phi^{(1)} = A e^{-i\mu x - \gamma_\mu y} + Q e^{\frac{ik_0 x}{1+M}} V(x, y; k_0) + \phi,$$

$$\phi^{(2)} = B e^{-i\mu x + \eta_\mu y} - Q e^{\frac{ik_0 x}{1+M}} V\left(x, y \sqrt{1+M^2}; \frac{k_0}{1-M^2}\right) + \psi,$$

$$\eta = d e^{-i\mu x} + \zeta,$$

... (4.3)

the time factor $\exp(-i\omega t)$ being understood throughout. Conditions on $y = 0, x < 0$ remain unaltered by the introduction of the new functions, so that, for a rigid plate, the equations (2.12) remain valid. Application

of/

of the conditions (2.2) and (2.3) on the vortex sheet leads, after Fourier transformation, to

$$\begin{aligned}
 -i\omega Z_+(s) &= \Phi'_+(s,0) - \frac{Q(2k_0)^{1/2} G_0}{(s+k_0)^{1/2}}, \\
 -i\omega D_s Z_+(s) &= \Psi'_+(s,0) + \frac{Q(2k_0)^{1/2} G_0}{\left(s + \frac{k_0}{1+M}\right)^{1/2}} - U_d, \\
 &\dots (4.4)
 \end{aligned}$$

$$\begin{aligned}
 D_s \Psi_+(s,0) &= \frac{iU\psi_0}{\omega} - \Phi'_+(s,0) \\
 &= \frac{iQG_0}{(s+k_0)} + \frac{iQG_0}{(1+M)\left(s + \frac{k_0}{1+M}\right)},
 \end{aligned}$$

in which $G_0 = \int_0^\infty \exp(2it^2) dt = \frac{1}{2} \left(\frac{\pi i}{2}\right)^{1/2}$. The relations (2.10) remain

valid, and the Wiener-Hopf equation replacing (2.13) is found to be

$$-i\omega Z_+(s) = K(s) F_-(s) + \frac{i\gamma_\mu A}{s-\mu} + N(s) \quad \dots (4.5)$$

in which $K(s)$ is defined in (2.14), $F_-(s)$ in (3.3) and the new function $N(s)$ is given by

$$\begin{aligned}
 N(s) &= \left(\frac{D_s K(s)}{w_s} \right) \frac{Q(2k_0)^{1/2} G_0}{\left(s + \frac{k_0}{1+M}\right)^{1/2}} - \left(\frac{K(s)}{y_s} \right) \frac{Q(2k_0)^{1/2} G_0}{(s+k_0)^{1/2}} \\
 &+ \frac{iK(s)QG_0}{(s+k_0)} + \frac{iK(s)QG_0}{(1+M)\left(s + \frac{k_0}{1+M}\right)}. \quad \dots (4.6)
 \end{aligned}$$

A solution can be obtained in the low Mach number limit using the factorisation (2.17). By examining the form of $Z_+(s)$ as $s \rightarrow \infty$,

Im $s > 0$, one can deduce the form of $\zeta(x)$ as $x \rightarrow 0+$. The terms $O(s^{-1})$ and $O(s^{-2})$ in the asymptotic development of $Z_+(s)$ give contributions to $\zeta(x)$ which are $O(1)$ and $O(x)$ respectively, and these

make no contribution to the total deflexion $\eta(x)$, being cancelled exactly by terms in the expansion of $de^{-i\mu x}$ (cf. 4.3). $Z_+(s)$ also contains a term $O(s^{-3/2})$, corresponding to $\eta(x) = O(x^{1/2})$, and the full Kutta condition requires that the coefficient of this term vanish. Thus one determines Q as $2A(2\mu/\pi k_0)^{1/2}$, and then $\eta(x) = O(x^{3/2})$ so that the vortex sheet leaves the plate with zero gradient. The value of Q quoted above is less than that given by Orszag and Crow (1970) by a factor $2^{-1/2}$ (allowing for slight differences of notation), but the precise value is not particularly important.

With Q determined as above, the far-field form of $\phi(r, \theta)$ can be found as

$$\phi(r, \theta) \sim - \left(\frac{1}{\pi k_0 r} \right)^{1/2} e^{ik_0 r + i\pi/4} A \left(\frac{\mu}{k_0} \right)^{1/2} \operatorname{cosec} \theta/2,$$

to which, according to (4.3), should be added

$$- \frac{Q \exp(ik_0 r)}{2i (k_0 r)^{1/2}} \operatorname{cosec} \theta/2,$$

to obtain the total scattered potential in $y > 0$ (except, of course, near the vortex sheet $\theta = 0$),

$$\begin{aligned} \phi_{\text{total}} &\sim - \left(\frac{2}{\pi k_0 r} \right)^{1/2} A \left(\frac{\mu}{k_0} \right)^{1/2} e^{ik_0 r} \operatorname{cosec} \theta/2 \\ &= - \left(\frac{2^{3/2}}{\pi k_H r} \right)^{1/2} e^{ik_0 r + 3\pi i/8} \left(\frac{A}{M} \right) \operatorname{cosec} \theta/2 \end{aligned} \quad \dots (4.7)$$

The radiated density fluctuation is

$$\rho' \sim \rho_0 \left(\frac{\ell}{r} \right)^{1/2} M \operatorname{cosec} \theta/2, \quad \dots (4.8)$$

and the intensity-directivity law is

$$I \sim U^2 \operatorname{cosec}^2 \theta/2. \quad \dots (4.9)$$

Thus imposition of the full Kutta condition results in an increase of the radiated intensity by a factor M^{-2} , and a very substantial change in the directivity pattern. The velocity exponent in (4.9) is the lowest yet found in aerodynamic noise theory; even a two-dimensional monopole gives only $I \sim U^3$ (Ffowcs Williams, 1969). The reason for the very

high/

high acoustic efficiency of the flow with full Kutta condition is to be found simply in the form of the new term involving Q in (4.3) and the correction function ϕ which it induces. These new terms are essentially acoustic in nature, and their amplitude near the plate edge is at least comparable with that of the essentially hydrodynamic small-scale motion discussed in Section 2. Consequently, it is hardly surprising that a motion coherent on the wavelength scale ℓM^{-1} should be more efficient than the hydrodynamic motion on the much smaller scale ℓ .

We do not claim that a radiation efficiency as high as that predicted by (4.9) is ever likely to be observed in practice. The principal reason for giving the results of applying the full Kutta condition is that criticism has often been made of the scattering theories of Ffowcs Williams and Hall (1970) and Crighton and Leppington (1970, 1971), in which the velocity components are allowed to become infinite (though integrable) at the plate edge. These singularities apparently form an integral part of the theory (but see Crighton and Leppington, 1971) and it has been held against the theories that a removal of edge singularities by the imposition of a Kutta condition would very much reduce the scattered radiation. The example worked out in detail here shows that precisely the opposite is true. Application of a Kutta condition does not merely require a highly localised change in the flow, but the introduction, for an incompressible fluid, of a first-order change in the mean flow, or for a compressible flow, of a first-order motion varying on the wavelength scale. It is only to be expected that a large increase in the radiation should result from the introduction of such a highly organised flow.

5. The Diffraction Problem

We next give a brief discussion of the diffraction problem for the vortex sheet-rigid plate system. Suppose the incident field to take the form

$$\phi^{(1)} = \exp[-ik_0(x \cos \theta_0 + y \sin \theta_0)] ,$$

representing a monochromatic plane wave generated by a distant source in the stagnant fluid. In order to apply the Wiener-Hopf method, it is convenient to split off explicitly from the potentials $\phi^{(1)}$ and $\phi^{(2)}$ the waves which are reflected from, and transmitted through, the vortex sheet. (In fact this is necessary, since for complex $k_0 = k_1 + ik_2$ these waves would become exponentially large as $x \rightarrow +\infty$ for fixed y , and the domains of analyticity for the half-range Fourier transforms would not overlap to provide the necessary strip of analyticity for the full-range transforms.) Because of the assumed linearity of the problem, we may neglect instabilities of the vortex sheet, and later superpose the fields discussed in Sections 2 and 4 on the diffracted field to be examined here. Thus we now define

$$\begin{aligned} \phi^{(1)} &= e^{-ik_0(x \cos \theta_0 + y \sin \theta_0)} + R e^{-ik_0(x \cos \theta_0 - y \sin \theta_0)} + \phi, \\ \phi^{(2)} &= T e^{-ik_0 x \cos \theta_0 + w_\theta y} + \psi, \\ \eta &= h e^{-ik_0 x \cos \theta_0} + \zeta, \end{aligned} \quad \dots (5.1)$$

where the subscript θ in place of s on the functions D_s, w_s, γ_s is to imply their evaluation at $s = -k_0 \cos \theta_0$. The functions with coefficients R, T, h represent the reflected and transmitted waves and the vortex sheet deflexion under the incident field as if the vortex sheet were doubly infinite. Application of the boundary conditions (2.2) and (2.3) for all x gives the solutions

$$\begin{aligned} R &= \frac{(1 + M \cos \theta_0)^2 \sin \theta_0 - \{(1 + M \cos \theta_0)^2 - \cos^2 \theta_0\}^{1/2}}{(1 + M \cos \theta_0)^2 \sin \theta_0 + \{(1 + M \cos \theta_0)^2 - \cos^2 \theta_0\}^{1/2}}, \\ T &= \frac{2 \sin \theta_0 (1 + M \cos \theta_0)}{(1 + M \cos \theta_0)^2 \sin \theta_0 + \{(1 + M \cos \theta_0)^2 - \cos^2 \theta_0\}^{1/2}}, \\ h &= \frac{2 \sin \theta_0}{a_0} \frac{\{(1 + M \cos \theta_0)^2 - \cos^2 \theta_0\}^{1/2}}{(1 + M \cos \theta_0)^2 \sin \theta_0 + \{(1 + M \cos \theta_0)^2 - \cos^2 \theta_0\}^{1/2}} \end{aligned} \quad \dots (5.2)$$

which are real and finite for all θ_0 provided $M < 1$.

For $\pi - \theta_0 < \theta < \pi$, the field ϕ must be such as to change the coefficient R to unity, representing the wave reflected from the rigid plate, while in the shadow region below the plate, the field ψ must annihilate the transmitted wave. Apart from these requirements, we assert that ϕ, ψ must represent outgoing diffracted fields at infinity (unstable modes being excluded here), and this assures the existence of a strip

$$-\frac{k_0}{1 + M} < \text{Im } s < + k_0 \cos \theta_0$$

for the Wiener-Hopf problem.

In place of (2.13) we now find the Wiener-Hopf functional equation

$$-i\omega Z_+(s) = K(s) F_-(s) - \frac{i w_\theta T}{D_\theta (s - k_0 \cos \theta_0)}, \quad \dots (5.3)$$

with solutions

$$i\omega Z_+(s) = \frac{i w_\theta T}{D_\theta (s - k_0 \cos \theta_0)} \left(1 - \frac{K_+(s)}{K_+(k_0 \cos \theta_0)} \right),$$

$$\phi(s,0) = - \frac{i w_\theta T}{\gamma_s D_\theta (s - k_0 \cos \theta_0)} \frac{K_+(s)}{K_+(k_0 \cos \theta_0)}, \quad \dots (5.4)$$

$$\psi(s,0) = \frac{i w_\theta T}{w_s (s - k_0 \cos \theta_0)} \frac{D_s}{D_\theta} \frac{K_+(s)}{K_+(k_0 \cos \theta_0)}.$$

Fourier inversion and deformation of the path of integration onto the path of steepest descent splits the fields naturally into geometrical optics fields of the obvious kinds plus cylindrical diffracted waves emanating from the plate edge. For $M \ll 1$ the distant fields are essentially the same as in Sommerfeld's classical diffraction problem (Noble, 1958, p.57). This follows since, provided $s/k_0 = O(1)$ as $M \rightarrow 0$, the kernel $K(s)$ tends to the Sommerfeld kernel $2\gamma_s$, and the far-fields are determined solely by the matched acoustic wavenumber (i.e. by $s = -k \cos \theta$ for ϕ , for example). The limiting value of $K(s)$ is not approached uniformly in s , however, and the field behaviour near the plate edge is fundamentally different from that in the Sommerfeld case. In fact, if M is small but non-zero, it can be shown from (5.4) that

$$\begin{aligned} \eta(x) &= O(x^{1/2}), \\ \phi(x) &= O(|x|^{3/2}), \\ \psi(x) &= O(|x|^{1/2}), \end{aligned} \quad \dots (5.5)$$

near $\underline{x} = 0$. The velocity components in the stagnant fluid thus remain finite at the edge, in contrast with the case $M = 0$ in which they become infinite like $|\underline{x}|^{-1/2}$. In the absence of any Kutta condition, however, the velocity components below the sheet still have (integrable) singularities.

The "full" Kutta condition of Section 4 can be imposed if we superpose the solution of Section 2, consisting of a Helmholtz instability on a doubly-infinite vortex sheet plus the correction due to the plate. Using the notation of Section 2, it can be shown that if we choose

$$A = \frac{w_\theta T K_+(\mu)}{D_\theta \gamma_\mu K_+(k_0 \cos \theta_0)} \quad \dots (5.6)$$

then/

then

$$\begin{aligned} \eta(\underline{x}) &= O(x^{3/2}) , \\ \phi(\underline{x}) &= O(|\underline{x}|^{5/2}) , \\ \psi(\underline{x}) &= O(|\underline{x}|^{3/2}) , \end{aligned} \quad \dots (5.7)$$

ensuring that the vortex sheet leaves the plate with zero gradient, and that all velocity components remain finite near the plate edge. This superposition does not, of course, represent the only solution of the problem, for there exist eigensolutions, which may or may not satisfy the full Kutta condition, of the kinds discussed in Sections 2 and 4. However, the unstable mode with A determined in (5.6) may perhaps be legitimately regarded as causally induced by the incident field, although it has no appreciable effect on the distant sound field. For the only genuine acoustic part of the unstable mode is that part induced by the presence of the plate and given in (2.18). Using (5.6) it can be seen that the amplitude of this scattered field is smaller than that of Sommerfeld's diffracted field by a factor of order M . We conclude that the effect of the vortex sheet at small Mach numbers is to smooth the behaviour near the plate edge at the expense of exciting a non-radiating Helmholtz instability, with negligible change in the far-field radiation.

6. Discussion and Conclusions

This paper has examined the low Mach number radiation from a flow coupled to an inhomogeneous solid surface. Very few systems of this kind appear to be amenable to calculation, even within the confines of linear inviscid hydrodynamics, and the example followed through here seems to be the first involving a surface which is non-compact relative to the acoustic wavelength.

Before mentioning the possible relevance of the detailed results of this paper, particularly those of Section 2, we must acknowledge a number of points on which the model flow studied must be criticised. In the first place, as noted in Section 2, the notion of a spatially growing instability has its difficulties in an elliptic problem. Linearisation is not valid everywhere in space, and departures from linear behaviour downstream of the trailing edge might, for elliptic governing equations, have a significant effect everywhere, even in the region where linearisation is apparently valid. Nonetheless, as Orszag and Crow (1970) remark, there is considerable experimental confirmation of theories based on the idea of spatial instability, so that the linear theory predictions may be adequate in the regions where one might casually expect them to be. To that extent, the predictions of Orszag and Crow regarding the influence of the plate on the shape of the eigenfunctions of the vortex sheet - that such influence vanishes essentially for $k_H |\underline{x}| \gtrsim 1$ - must then be correct. Here, however, we are not merely concerned with the flow pattern for $|\underline{x}| \lesssim k_H^{-1}$ but for the much larger region $|\underline{x}| \lesssim k_0^{-1}$, for scattering theory leads us to expect that appreciable conversion of eddy energy into propagating sound will occur from the interaction of the plate edge with fluid elements up to an acoustic wavelength from the edge. Within this distance, however, the vortex sheet amplitude has grown by a factor $\exp(M^{-1})$, and the

linearised/

linearised solution can have no possible relevance. This argument, however, overstates the case against the model. In Section 2, the field is split into that of a doubly-infinite vortex sheet plus a correction due to the plate, the latter vanishing for $k_H |\underline{x}| \gtrsim 1$. Presumably the effect of the plate is properly accounted for by such a split. The field generated by flow at distances greater than k_H^{-1} from the edge is the same as that generated if no plate were present and must, if non-linear terms could be included, give an intensity varying as U^6 (Lighthill, 1952).

The important results of Section 2, for a rigid plate, are the low velocity exponent $I \sim U^6$ for three dimensions, and the pronounced forward directivity $I \sim \sin^2 \theta/2$. According to Section 3, these results are not greatly changed by compliance of the plate. In the case of a limp plate, the velocity index is increased to 6 and the directivity maximum shifted from the extreme forward direction $\theta = \pi$ to the broadside direction $\theta = \pi/2$. These results are not dependent upon details of the flow (Crighton and Leppington 1970, 1971), and also not particularly sensitive to geometry, so that they represent features which should be possessed by the sound field resulting from the interaction of a cylindrical shear layer with a jet engine tailpipe.

To demonstrate the importance of the surface scattered noise, suppose that the flow downstream of the plate edge becomes turbulent at distances greater than $k_H^{-1} = \ell$, with r.m.s. velocity level u , and that the turbulent region consists of a large plane sheet of thickness ℓ and area S . Then from Lighthill's (1952) solution

$$\rho'(\underline{x}, t) = \frac{\rho_0}{4\pi a_0^4 |\underline{x}|} \frac{\partial^2}{\partial t^2} \int u_i u_j \left(\underline{y}, t - \frac{|\underline{x}|}{a_0} \right) dy$$

one can show that the intensity radiated from the turbulent flow is

$$I_Q \sim \rho_0 U^3 S |\underline{x}|^{-2} M^5 \left(\frac{u}{U} \right)^6 \dots (6.1)$$

Here we have assumed the fluctuating part of $u_i u_j$ to be of order Uu , and noted that the frequency associated with the quadrupole field is u/ℓ , rather than U/ℓ the frequency of the shear layer instability (this is a point repeatedly emphasized by Lighthill, 1954). To be consistent, we must then also take the A of (2.18) to be of order $u\ell$, so that the velocities induced by the instability become of order u at distances $O(\ell)$ downstream from the edge. With the appropriate modification of (2.20) for three dimensions, the ratio of quadrupole intensity to surface scattered intensity is

$$M^3 (u/U)^4 S \ell^{-2} \dots (6.2)$$

Even with $M = \frac{1}{2}$, $(u/U) = \frac{1}{4}$, extreme values, it is quite clear that the area S must span at least 100 correlation areas ℓ^2 in order for the quadrupole contribution to approach that created by surface scattering.

Thus/

Thus the interaction of shear layer instability with a large surface has the following characteristics; (1) a frequency spectrum concentrated on the frequency U/ℓ , a value higher than that of free turbulence by a factor U/u ; (2) a velocity exponent for the intensity between 5 and 6; (3) an extremely pronounced forward directivity; (4) a total radiated power at least comparable with that of turbulence-generated noise unless the turbulent volume is very large.

Attributes of precisely this kind go a long way toward explaining certain discrepancies which exist between the measured noise field of current turbofan and turbojet engines and predictions based on Lighthill's theory of convected quadrupoles with surface effects ignored. The situation - the so-called "excess noise" problem - is not well documented in the open literature, but appears to involve the following behaviour. For angles less than $\pi/2$ from the exhaust flow direction, the correlation of experimental data using the results of Lighthill's theory is quite adequate over a wide variety of engine types and operating conditions. In the forward directions, however, substantial deviations occur, for which as yet we have no satisfactory correlation and prediction techniques. The frequency spectrum for forward emission has two peaks, with comparable contributions to the total intensity from the spectral regions around each of the peaks. The contribution to the intensity associated with the lower of the two frequencies continues to scale according to Lighthill's theory. That associated with the higher frequency does not, involving in particular a velocity exponent somewhere between 4 and 6.

We make the tentative suggestion that the above behaviour can be explained on the basis of the predictions of this paper. The two frequencies are to be identified with u/ℓ , the frequency of eddy motion in a convected reference frame, and U/ℓ , the frequency associated with the most rapidly growing mode of shear layer instability. Sound at frequencies around u/ℓ is generated by eddies in the fully turbulent mixing region downstream of the jet exit plane. That at frequencies around U/ℓ is generated by the interaction, with the engine tailpipe, of growing modes on the annular shear layer immediately aft of the exit plane, and has a very definite forward directivity. In the forward directions, the two fields are of comparable magnitude, even for values of M approaching unity, in view of the strong dependence of (6.2) upon the ratio (u/U) .

Of course, this may not be the only mechanism responsible, and a more detailed assessment of the claim made here must rest upon results of more refined experiment and theory. Obviously, a first step would be to determine more precisely the values of the two peak frequencies observed in practice, and to determine whether or not the "excess noise" directivity agrees at all with the $\sin^2 \theta/2$ pattern predicted here. Under certain circumstances, the geometry of the annular shear layer might also be expected to play a part capable of experimental detection. Since the problem of the annular shear layer has its own analytical interest, as well as more direct correspondence with practice than the model used here, we defer consideration of it to a subsequent paper.

The author gratefully acknowledges the support provided by a contract from the Ministry of Technology, administered by the National Gas Turbine Establishment, Pyestock, Hampshire.

References

- R. Amiet and W. R. Sears J. Fluid Mech. 44, 227. 1970.
- D. G. Crighton and F. G. Leppington J. Fluid Mech. 43, 721. 1970.
- D. G. Crighton and F. G. Leppington J. Fluid Mech. 46, 557. 1971.
- S. C. Crow Studies in Appl. Math. XLIX/1, 21. 1970.
- N. Curle Proc. Roy. Soc. A. 231, 505. 1955.
- H. G. Davies J. Fluid Mech. 43, 597. 1970.
- J. E. Ffowcs Williams J. Acoust. Soc. Am. 35, 930. 1963.
- J. E. Ffowcs Williams J. Fluid Mech. 22, 347. 1965.
- J. E. Ffowcs Williams Annual Review of Fluid Mechanics 1, (ed. W. R. Sears), 197. 1969.
- J. E. Ffowcs Williams and L. H. Hall J. Fluid Mech. 40, 657. 1970.
- M. Heckl Private communication. 1970.
- M. S. Howe J. Fluid Mech. 43, 353. 1970.
- H. Lamb Proc. London Math. Soc. (2) 4, 190. 1907.
- M. J. Lighthill Proc. Roy. Soc. A. 211, 564. 1952.
- M. J. Lighthill Proc. Roy. Soc. A. 222, 1. 1954.
- W. C. Meecham J. Acoust. Soc. Am. 35, 116 and 931. 1963.
- B. Noble "Methods based on the Wiener-Hopf technique". London; Pergamon. 1958.
- F. Obermeier Acustica 18, 238. 1967.
- S. A. Orszag and S. C. Crow Studies in Appl. Math. XLIX/2, 167. 1970.
- A. Powell J. Acoust. Soc. Am. 35, 731. 1963.
-

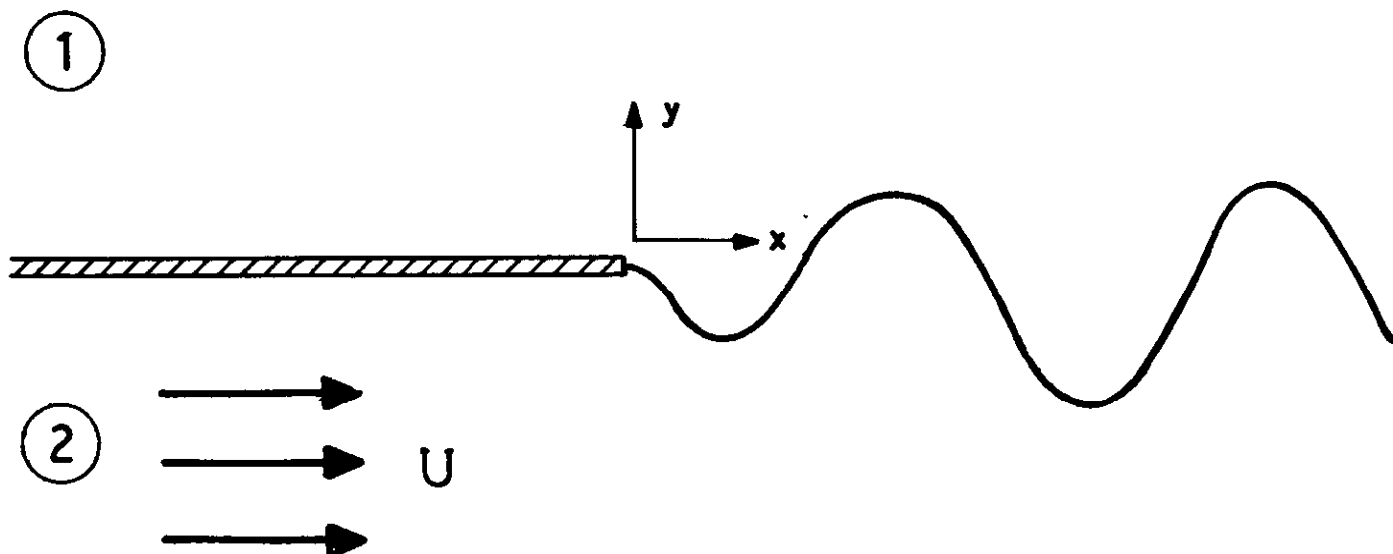


Fig. 1 Vortex sheet leaving a plate and undergoing a spatial instability. In the unperturbed state the fluid in region 1 (above the plate) is stagnant, while that in region 2 (below the plate) streams with uniform velocity $(U, 0)$.

Chapter 4

Diffraction Radiation

by

H. Levine,
Department of Mathematics,
Stanford University, California;
Visiting Professor, Department of Mathematics,
Imperial College, London

In their considerations relative to aerodynamic noise Crighton and Leppington discuss the output of fixed acoustical sources with time-periodic strength which are located near the edge of a semi-infinite plane; and find the scattered wave amplitude to exceed that of the primary source in the far field, the amplification being greater for quadrupoles than dipoles. If localised sources with an invariable strength are in uniform rectilinear motion at subsonic speed past the edge, there is no primary radiation and only indirect or diffraction radiation whose time-varying sources are continuously distributed over the plane. Such radiation is emitted when the source is near to the impact (or minimum) distance from the edge, and the total amount of energy radiated depends on the source strength and polarization, the Mach number and impact distance; it is the variation with impact distance d and Mach number M that claims principal interest and reflects the specific nature of the radiation phenomenon.

The inhomogeneous linear wave equation for density fluctuations,

$$\left(\frac{\partial^2}{\partial t^2} - c^2 \nabla^2 \right) \rho(r, t) = \frac{\partial Q}{\partial t} - \frac{\partial F_i}{\partial x_i} + \frac{\partial^2 T_{ij}}{\partial x_i \partial x_j}$$

contains a trio of source terms, pertaining to the introduction of mass at the rate $Q(r, t)$, the application of a force $\vec{F}(r, t)$ with components F_i and the action of stresses with components T_{ij} , all per unit volume.

It is noteworthy that first order partial derivatives of the scalar and vector functions Q, \vec{F} enter, whereas double differentiation of the tensor \vec{T} occurs. The total energy radiated, ϵ , is conveniently found from the power expended in maintaining the appropriate primary source in its state of motion, and has the respective forms

$$\epsilon_{\text{source}} = \frac{c^2}{\rho_0} \int \rho_s(r, t) Q(r, t) dr dt$$

$$\epsilon_{\text{dipole}} = \int \nabla \phi_s(r, t) \cdot \vec{F}(r, t) dr dt$$

$$\epsilon_{\text{quadrupole}} = - \int \nabla \phi_s(r, t) \cdot \nabla \cdot \vec{T}(r, t) dr dt$$

where/

where the density and velocity potential of the secondary sources on the plane are linked by

$$\rho_s(r,t) = - \frac{\rho_0}{c^2} \frac{\partial \phi_s(r,t)}{\partial t}$$

and ρ_0 is the uniform equilibrium density. When the source moves in a plane which is transverse to the straight edge, it appears that

$$\epsilon_{\text{source}} = \frac{Q_0^2}{\rho_0 d} \mathcal{F}_0(M)$$

$$\epsilon_{\text{dipole}} = \frac{\mathcal{F}_1(M, F_1^2)}{\rho_0 c^2 d}$$

and

$$\epsilon_{\text{quadrupole}} = \frac{\mathcal{F}_2(M, T_{ij}^2)}{\rho_0 c^2 d^3},$$

with a singular behaviour for each of the functions $\mathcal{F}_{0,1,2}$ in the limit $M \rightarrow 1$; specifically, in the case of a simple source of fixed strength Q_0 ,

$$\mathcal{F}_0(M) = \frac{1}{32\pi} \frac{M^2}{(1-M^2)^{3/2}},$$

independently of the angle of the trajectory, and for a dipole with moment F in the plane of the trajectory,

$$\mathcal{F}_1(M, F_1^2) = \frac{F^2}{32\pi} \left[\frac{\cos^2 \theta}{(1-M^2)^{3/2}} + 2 \frac{\sin^2 \theta}{M^2} \left(\frac{1}{\sqrt{1-M^2}} - 1 \right) \right]$$

where θ denotes the angle between its axis and the direction of motion.

To illustrate the indicated style of calculation, consider a quadrupole source moving, in the plane $x_2 = 0$, with velocity V along the x_3 -direction and passing at a distance d from the edge of a half-plane occupying the region $x_1 > 0$, $-\infty < x_2 < \infty$, $x_3 = 0$.

Writing

$$T_{ij} = Q_{ij} \delta(x_1 + d) \delta(x_2) \delta(x_3 - Vt)$$

the primary source function, expressed in multiple Fourier integral fashion, takes the form

$\rho_0 /$

$$\rho_0(r, t) = \frac{1}{(2\pi)^4 c^3} \int_{-\infty}^{\infty} \frac{e^{i\zeta_1(x_1-x'_1)+i\zeta_2(x_2-x'_2)+i\zeta_3(x_3-x'_3)-i\omega(t-t')}}{\zeta_1^2 + \zeta_2^2 + \zeta_3^2 - \left(\frac{\omega}{c}\right)^2}$$

$$\frac{\partial^3 T_{ij}}{\partial x'_i \partial x'_j} dx'_1 dx'_2 dx'_3 dt' d\zeta_1 d\zeta_2 d\zeta_3 d\omega$$

$$= - \frac{1}{(2\pi)^3 c^3 V} \int_{-\infty}^{\infty} \left\{ Q_{11} \zeta_1^2 + 2Q_{12} \zeta_1 \zeta_2 + Q_{22} \zeta_2^2 \right\}$$

$$\frac{e^{i\zeta_1(x_1+d)+i\zeta_2 x_2 + i\omega\left(\frac{x_3}{V} - t\right)}}{\zeta_1^2 + \zeta_2^2 + \left(\frac{\omega}{V}\right)^2 - \left(\frac{\omega}{c}\right)^2} d\zeta_1 d\zeta_2 d\omega$$

$$- \frac{1}{(2\pi)^3 c^3 V} \int_{-\infty}^{\infty} \left\{ 2Q_{13} \zeta_1 \frac{\omega}{V} + 2Q_{23} \zeta_2 \frac{\omega}{V} + Q_{33} \left(\frac{\omega}{V}\right)^2 \right\}$$

$$\frac{e^{i\zeta_1(x_1+d)+i\zeta_2 x_2 + i\omega\left(\frac{x_3}{V} - t\right)}}{\zeta_1^2 + \zeta_2^2 + \left(\frac{\omega}{V}\right)^2 - \left(\frac{\omega}{c}\right)^2} d\zeta_1 d\zeta_2 d\omega$$

and complies with the requirement of causality if ω has an infinitesimal positive imaginary part. If the screen is limp and cannot support any pressure or density fluctuations, the secondary source distribution thereupon may be expressed in the product form $f(x_1, x_2, t) \delta(x_3)$, $x_1 > 0$ and the concomitant density function elsewhere is

$$\rho_s(r,t) = - \frac{1}{(2\pi)^4 c^3} \int_{-\infty}^{\infty} \frac{e^{i\zeta_1 x_1 + i\zeta_2 x_2 + i\zeta_3 x_3 - i\omega t}}{\zeta_1^2 + \zeta_2^2 + \zeta_3^2 - \left(\frac{\omega}{c}\right)^2} f(\zeta_1, \zeta_2, \omega) d\zeta_1 d\zeta_2 d\zeta_3 d\omega$$

$$= - \frac{i\pi}{(2\pi)^4 c^3} \int_{-\infty}^{\infty} \frac{e^{i\zeta_1 x_1 + i\zeta_2 x_2 + i\sqrt{(\omega/c)^2 - \zeta_1^2 - \zeta_2^2} |x_3| - i\omega t}}{\sqrt{(\omega/c)^2 - \zeta_1^2 - \zeta_2^2}} f(\zeta_1, \zeta_2, \omega) d\zeta_1 d\zeta_2 d\omega$$

with the transform

$$f(\zeta_1, \zeta_2, \omega) = \int_0^{\infty} e^{-i\zeta_1 x_1} dx_1 \int_{-\infty}^{\infty} e^{i\zeta_2 x_2} dx_2 \int_{-\infty}^{\infty} e^{i\omega t} f(x_1, x_2, t) d\omega$$

that is analytic in the lower half of the ζ_1 - plane.

An explicit characterization of the latter function obtains from the transform relation

$$\frac{f(\zeta_1, \zeta_2, \omega)}{i\sqrt{\left(\frac{\omega}{c}\right)^2 - \zeta_1^2 - \zeta_2^2}} = \frac{2}{V} \left\{ Q_{11} \zeta_1^2 + 2Q_{12} \zeta_1 \zeta_2 + Q_{22} \zeta_2^2 + 2Q_{13} \zeta_1 \frac{\omega}{V} + 2Q_{23} \zeta_2 \frac{\omega}{V} + Q_{33} \frac{\omega^2}{V^2} \right\} \frac{e^{i\zeta_1 d}}{\zeta_1^2 + \zeta_2^2 + \gamma_0^2}$$

$$= g(\zeta_1, \zeta_2, \omega), \quad \gamma_0^2 = \left(\frac{\omega}{V}\right)^2 - \left(\frac{\omega}{c}\right)^2$$

that is consequent to the requirement

$$\rho_0(r,t) + \rho_s(r,t) = 0, \quad x_1 > 0, \quad -\infty < x_2 < \infty, \quad x_3 = 0$$

and involves a second unknown function $g(\zeta_1, \zeta_2, \omega)$ which has an analytic character in the upper half of the ζ_1 - plane and is related to the density on the domain $x_1 < 0, -\infty < x_2 < \infty, x_3 = 0$. By recasting the transform relation in terms of components which are regular in the respective halves of the ζ_1 - plane, it follows that

$f(\zeta_1, \zeta_2, \omega)$

$$\frac{-Q_{11}(\zeta_2^2 + \gamma_0^2) + 2iQ_{12}\zeta_2 \sqrt{\zeta_2^2 + \gamma_0^2} + Q_{22}\zeta_2^2 + 2iQ_{13} \frac{\omega}{V} \sqrt{\zeta_2^2 + \gamma_0^2} + 2Q_{23} \zeta_2 \frac{\omega}{V} + Q_{33} \frac{\omega^2}{V^2}}{V \sqrt{\zeta_2^2 + \gamma_0^2} (\zeta_1 - i \sqrt{\zeta_2^2 + \gamma_0^2})}$$

$$\cdot e^{-\sqrt{\zeta_2^2 + \gamma_0^2} x_2} \sqrt{\sqrt{\frac{\omega^2}{c^2} - \zeta_2^2} + i \sqrt{\zeta_2^2 + \gamma_0^2}} \sqrt{\sqrt{\frac{\omega^2}{c^2} - \zeta_2^2} - \zeta_1}$$

Employing the representation

$$\phi_s(r, t) = \frac{1}{(2\pi)^4 \rho_0} \int_{-\infty}^{\infty} \frac{e^{i\zeta_1 x_1 + i\zeta_2 x_2 + i\zeta_3 x_3 - i\omega t}}{\omega \left\{ \zeta_1^2 + \zeta_2^2 + \zeta_3^2 - \left(\frac{\omega}{c} \right)^2 \right\}} f(\zeta_1, \zeta_2, \omega) d\zeta_1 d\zeta_2 d\zeta_3 d\omega$$

the rate of energy radiation may be written as

$$\begin{aligned} \dot{W} &= - \int \nabla \phi_s \cdot \nabla \cdot \bar{T} dx_1 dx_2 dx_3 \\ &= - \int \left\{ \frac{\partial \phi_s}{\partial x_1} \left(\frac{\partial T_{11}}{\partial x_1} + \frac{\partial T_{21}}{\partial x_2} + \frac{\partial T_{31}}{\partial x_3} \right) + \frac{\partial \phi_s}{\partial x_2} \left(\frac{\partial T_{12}}{\partial x_1} + \frac{\partial T_{22}}{\partial x_2} + \frac{\partial T_{32}}{\partial x_3} \right) \right. \\ &\quad \left. + \frac{\partial \phi_s}{\partial x_3} \left(\frac{\partial T_{13}}{\partial x_1} + \frac{\partial T_{23}}{\partial x_2} + \frac{\partial T_{33}}{\partial x_3} \right) \right\} dx_1 dx_2 dx_3 \\ &= \int \left\{ Q_{11} \frac{\partial^2 \phi_s}{\partial x_1^2} + 2Q_{12} \frac{\partial^2 \phi_s}{\partial x_1 \partial x_2} + Q_{22} \frac{\partial^2 \phi_s}{\partial x_2^2} + 2Q_{13} \frac{\partial^2 \phi_s}{\partial x_1 \partial x_3} + 2Q_{23} \frac{\partial^2 \phi_s}{\partial x_2 \partial x_3} \right. \\ &\quad \left. + Q_{33} \frac{\partial^2 \phi_s}{\partial x_3^2} \right\} \\ &\quad \cdot \delta(x_1 + a) \delta(x_2) \delta(x_3 - vt) dx_1 dx_2 dx_3 \end{aligned}$$

$$= - \frac{i}{(2\pi)^4 \rho_0} \int_{-\infty}^{\infty} \frac{Q_{11}\zeta_1^2 + 2Q_{12}\zeta_1\zeta_2 + Q_{22}\zeta_2^2 + 2Q_{13}\zeta_1\zeta_3 + 2Q_{23}\zeta_2\zeta_3 + Q_{33}\zeta_3^2}{\omega \left\{ \zeta_1^2 + \zeta_2^2 + \zeta_3^2 - \left(\frac{\omega}{c} \right)^2 \right\}} e^{-i\zeta_1 d} \cdot e^{i(\zeta_3 V - \omega)t} f(\zeta_1, \zeta_2, \omega) d\zeta_1 d\zeta_2 d\zeta_3 d\omega$$

and thus

$$\epsilon = - \frac{i}{(2\pi)^3 \rho_0 V}$$

$$\int_{-\infty}^{\infty} \frac{Q_{11}\zeta_1^2 + 2Q_{12}\zeta_1\zeta_2 + Q_{22}\zeta_2^2 + 2Q_{13}\zeta_1 \frac{\omega}{V} + 2Q_{23}\zeta_2 \frac{\omega}{V} + Q_{33} \frac{\omega^2}{V^2}}{\omega \left\{ \zeta_1^2 + \zeta_2^2 + \gamma_0^2 \right\}} e^{-i\zeta_1 d} \cdot f(\zeta_1, \zeta_2, \omega) d\zeta_1 d\zeta_2 d\omega$$

$$= - \frac{i\pi}{(2\pi)^3 \rho_0 V}$$

$$\int_{-\infty}^{\infty} \frac{-Q_{11}(\zeta_2^2 + \gamma_0^2) - 2iQ_{12}\zeta_2 \sqrt{\zeta_2^2 + \gamma_0^2} + Q_{22}\zeta_2^2 - 2iQ_{13} \frac{\omega}{V} \sqrt{\zeta_2^2 + \gamma_0^2} + 2Q_{23}\zeta_2 \frac{\omega}{V} + Q_{33} \frac{\omega^2}{V^2}}{\omega \sqrt{\zeta_2^2 + \gamma_0^2}}$$

$$\cdot e^{-\sqrt{\zeta_2^2 + \gamma_0^2} d} f\left(-i\sqrt{\zeta_2^2 + \gamma_0^2}, \zeta_2, \omega\right) d\zeta_2 d\omega$$

when the ζ_1 - integral is evaluated by closure of the contour in the lower half of the plane. Substituting the explicit form of $f(\zeta_1, \zeta_2, \omega)$ and having regard for the sign of the imaginary part of ω , one finds

$$\epsilon = /$$

$$\epsilon = \frac{1}{2(2\pi)^2 \rho_0 V^2} \operatorname{Re} \int_0^\infty \frac{d\omega}{\omega} \int_{-\infty}^\infty d\zeta_2 \frac{e^{-2\sqrt{\zeta_2^2 + \gamma_0^2} d}}{(\zeta_2^2 + \gamma_0^2)^{3/2}} \left\{ \sqrt{\frac{\omega^2}{c^2} - \zeta_2^2 + 1} \sqrt{\zeta_2^2 + \gamma_0^2} \right\} \\ \cdot \left\{ \left[-Q_{11}(\zeta_2^2 + \gamma_0^2) + Q_{22} \zeta_2^2 + 2Q_{23} \zeta_2 \frac{\omega}{V} + Q_{33} \frac{\omega^2}{V^2} \right]^2 \right. \\ \left. + 4(\zeta_2^2 + \gamma_0^2) \left[Q_{12} \zeta_2 + Q_{13} \frac{\omega}{V} \right]^2 \right\}$$

and after making the change of variable $\zeta_2 = \frac{\omega}{c} \tau$,

$$\epsilon = \frac{1}{2(2\pi)^2 \rho_0 V^3 c^2} \int_0^\infty \omega^2 d\omega \int_{-1}^1 \frac{e^{-2\frac{\omega d}{V} \sqrt{1-M^2(1-\tau^2)}}}{[1-M^2(1-\tau^2)]^{3/2}} \sqrt{1-\tau^2} \\ \cdot \left\{ [Q_{33} + Q_{22} M^2 \tau^2 - Q_{11}(1-M^2(1-\tau^2))] + 2M\tau Q_{23} \right\}^2 \\ + 4[1-M^2(1-\tau^2)] [Q_{13} + Q_{12} M\tau]^2 \Big\} d\tau \\ = \frac{1}{4(2\pi)^2 \rho_0 c^2 d^3} \int_0^{\pi/2} \frac{\cos^2 \psi d\psi}{[1-M^2 \cos^2 \psi]^3} \left\{ [Q_{33} + Q_{22} M^2 \sin^2 \psi - Q_{11}(1-M^2 \cos^2 \psi)]^2 \right. \\ + 4M^2 Q_{23}^2 \sin^2 \psi + 4[1-M^2 \cos^2 \psi] \\ \left. \cdot [Q_{13} + Q_{12} M^2 \sin^2 \psi] \right\}$$

In the case of a longitudinal quadrupole, with Q_{33} alone different from zero,

$$\epsilon = \frac{Q_{33}^2}{64\pi} \frac{1}{\rho_0 c^2 d^3} \frac{1 - \frac{1}{4} M^2}{(1-M^2)^{5/2}}$$

Chapter 5

Scattering of Quadrupole Sources near the End of a Rigid Semi-Infinite Circular Pipe

by

F. G. Leppington
Department of Mathematics,
Imperial College, London

1. Introduction

The Lighthill (1952) theory of aerodynamic noise shows that a region of turbulence in an unbounded medium is acoustically equivalent to a volume distribution of quadrupole sources whose strength is essentially proportional to the Reynolds stress tensor $\rho u_i u_j$. On account of the relative inefficiency of such multipoles, as producers of sound waves at great distance from the source region, there is a tendency for the sound field to be greatly magnified if any scattering surfaces are present.

Such effects have been discussed by Curle (1955), Ffowcs Williams and Hall (1970), Crighton and Leppington (1971), and lead to modifications of the intensity law $I \propto U^8$, obtained by Lighthill for the far field intensity I against typical turbulence velocity U , for an unbounded flow. Curle (1955) shows that the influence of a (small) rigid obstacle is equivalent to a distribution of dipoles, whence $I \propto U^6$. The sound intensity is found to be increased even more effectively for quadrupole sources that are situated within about a wavelength of the sharp edge of a large obstacle, to give $I \propto U^5$: Ffowcs Williams and Hall (1970) deal with the thin semi-infinite half-plane, with generalisations provided by Crighton and Leppington (1971).

The object of the present work is to examine the distant sound field induced by a region of turbulence near a jet exit. For the sake of simplicity, the model problem chosen to represent this situation is that of a perfectly rigid semi-infinite circular pipe of radius a and negligible thickness. The problem is posed as one of diffraction theory with an incident quadrupole distribution assumed to be of known strength, with harmonic time dependence $e^{-i\omega t}$ taken throughout.

If the wavelength $\lambda = 2\pi c/\omega = 2\pi/k$ is small compared with the radius a of the pipe, then the arguments familiar in ray theory indicate that the sound field is asymptotically equal to that of the semi-infinite plate, for which the results are already known. Accordingly, attention is directed to the limit $ka \ll 1$, in which the waves are much longer than the radius.

In/

In formulating the problem, it is found convenient to use a reciprocity theorem to recast the problem into the simpler one of determining the field, near the pipe exit, induced by an appropriate plane wave excitation. Since the problem is not axially symmetric for general incidence, the potential function is written in the form of a Fourier series of modes whose dependence on the azimuthal angle ψ is trigonometrical. The boundary value problem for each mode can be solved by Fourier transformation along the direction of the pipe, using the Wiener-Hopf technique in the manner of Levine and Schwinger (1948). This procedure is briefly outlined in Section 2.

The formal solution is interpreted in Section 3 for the case of sources within a wavelength of the end of the pipe. It is found that the leading term is of order (ka) , compared with the incident field of order $(ka)^2$. This is very similar to the results of Curle (1955) for small finite bodies; it is quite different from that of a semi-infinite plate and that of a waveguide formed by two parallel semi-infinite plates. Furthermore, only the zeroth (axially symmetric) and the first mode contribute to this asymptotic estimate, the higher modes being of a higher order in the small parameter ka . The detailed dependence of the field on source position \underline{x} close to the pipe is complicated, though not of particular importance, and can be given in integral form. The dependence on the angular position (θ_0, ψ_0) of the observer at \underline{x}_0 , far from the source region, is simple and is given explicitly.

A few relevant properties of the functions that occur in the Wiener-Hopf analysis are described in Section 4.

2. Formulation and Exact Solution

A distribution of quadrupole sources of prescribed strength $Q_{ij}(\underline{x}) e^{-i\omega t}$ per unit volume is situated in the vicinity of the open end of a rigid semi-infinite circular pipe. Cylindrical polar co-ordinates (ρ, ψ, z) are chosen so that the pipe occupies the region $\rho = a, z \leq 0$; spherical polars (r, θ, ψ) based on the same origin at the centre of the exit plane are also used in the analysis that follows (Fig. 1)

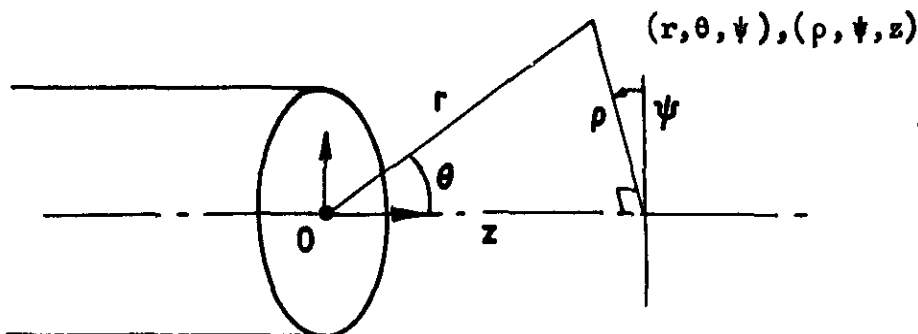


Fig. 1.
The geometry of the pipe, and the co-ordinate systems (r, θ, ψ) , (ρ, ψ, z) .

In order to calculate the sound field at an observation point \underline{x}_0 , we may confine our attention in the first instance to the problem of calculating the potential $G(\underline{x}; \underline{x}_0) e^{-i\omega t}$ induced at \underline{x}_0 by a single monopole source of unit strength at \underline{x} . The corresponding potential $\phi(\underline{x}_0) e^{-i\omega t}$ due to a quadrupole distribution of density $Q_{ij} e^{-i\omega t}$ follows

immediately/

immediately from the Green's function G , and is given by

$$\phi(\underline{x}_0) = \int Q_{ij} \frac{\partial^2 G}{\partial x_i \partial x_j}(\underline{x}; \underline{x}_0) d\underline{x}, \quad \dots (2.1)$$

evaluated over the whole source region.

The 'far field' limit of the potential G , when the observation point \underline{x}_0 is at great distance from the source region, is conveniently calculated by appealing to the reciprocal theorem, which states that $G(\underline{x}; \underline{x}_0) = G(\underline{x}_0; \underline{x})$. Thus the source and observation points may be interchanged, and in the limit $|\underline{x}_0| \rightarrow \infty$ we have to find the potential at \underline{x} due to a source at so great a distance that the incident field takes the form of a plane wave. Specifically, if the incident source potential is given by

$$G_i = \frac{\exp(ik|\underline{x} - \underline{x}_0|)}{|\underline{x} - \underline{x}_0|} \quad \dots (2.2)$$

then as $|\underline{x}_0| \rightarrow \infty$ we have

$$G_i \sim A \exp(-ik \underline{n} \cdot \underline{x}), \quad \dots (2.3)$$

$$\text{where } \underline{n} = \underline{x}_0 / |\underline{x}_0|, \text{ and } A = \exp(ik|\underline{x}_0|) / |\underline{x}_0| \quad \dots (2.4)$$

is regarded as a fixed parameter.

In the spherical co-ordinates (r, θ, ψ) of Fig. 1, the incident potential G_i of (2.3) has the plane wave form

$$G_i = A \exp \{-ikr(\cos \theta \cos \theta_0 + \sin \theta \sin \theta_0 \cos(\psi - \psi_0))\}, \quad \dots (2.5)$$

and we have to find the total potential G that satisfies

$$(\nabla^2 + k^2)G = 0 \quad \dots (2.6)$$

$$\text{with } \frac{\partial G}{\partial \rho} = 0 \quad \text{when } \rho = a, \quad z \leq 0. \quad \dots (2.7)$$

We have to solve (2.6, 2.7) together with a radiation condition, that $(G - G_i)$ behaves as an outgoing wave at large distance, and an edge condition that G and $\delta|\nabla G|$ remain finite for small values of the distance

δ from the edge (Fig. 2).

It is convenient to express the dependence on the azimuthal angle ψ as a Fourier cosine series; thus

$$G(\rho, \psi, z) = \frac{A}{2\pi} G^{(0)}(\rho, z) + \frac{A}{\pi} \sum_1^{\infty} G^{(n)}(\rho, z) \cos n(\psi - \psi_0), \quad \dots (2.8)$$

since the symmetry of the problem obviously implies that G is an even function of $(\psi - \psi_0)$.

The semi-infinite extent of the geometry ensures that the problem can be solved by means of Fourier transformation with respect to z and with use of the Wiener-Hopf technique, and the formal solution obtained in this manner by Levine and Schwinger (1948), Noble (1958), is described briefly in the following.

A small positive imaginary part k_2 is assigned to the wave number $k = k_1 + ik_2$, and we finally let $k_2 \rightarrow 0$. The complex Fourier transform $G^{(n)}(\rho, \alpha)$ of the mode $G^{(n)}(\rho, z)$ and the half range transforms $G_{\pm}^{(n)}$ are defined by the formulae

$$G^{(n)}(\rho, \alpha) = \int_{-\infty}^{\infty} G^{(n)}(\rho, z) e^{i\alpha z} dz = G_+^{(n)}(\rho, \alpha) + G_-^{(n)}(\rho, \alpha), \quad \dots (2.9)$$

where

$$G_-^{(n)} = \int_{-\infty}^0 G^{(n)}(\rho, z) e^{i\alpha z} dz, \quad G_+^{(n)} = \int_0^{\infty} G^{(n)}(\rho, z) e^{i\alpha z} dz. \quad \dots (2.10)$$

The form of the incident field, the boundary condition (2.7) and the radiation condition impose constraints on the possible values of the complex

variable α to ensure convergence of the integrals $G_+^{(n)}$ and $G_-^{(n)}$.

Specifically, it is found that $G_+^{(n)}$ is defined and analytic for $\text{im } \alpha > -k_2$, while $G_-^{(n)}$ is analytic for $\text{im } \alpha < k_2 \cos \theta_0$. The subscripts $+$ and $-$ are used here and henceforth to denote functions that are analytic in the respective regions $\text{im } \alpha > -k_2$ and $\text{im } \alpha < k_2 \cos \theta_0$.

It follows that the full range transform $G^{(n)} = G_+^{(n)} + G_-^{(n)}$ is analytic within the strip

$$-k_2 < \text{im } \alpha < k_2 \cos \theta_0, \quad \dots (2.11)$$

so that the inversion formula for $G^{(n)}(\rho, z)$ is given by

$$G^{(n)}/$$

$$G^{(n)}(\rho, z) = \frac{1}{2\pi} \int_{-\infty+ib}^{\infty+ib} G^{(n)}(\rho, \alpha) e^{-i\alpha z} d\alpha, \quad \dots (2.12)$$

where b lies between $-k_0$ and $+k_0 \cos \theta_0$.

The transform $G^{(n)}(\rho, \alpha)$ is found from equations (2.6), (2.8) and (2.9) to satisfy the equation

$$\rho^2 \frac{\partial^2 G^{(n)}}{\partial \rho^2} + \rho \frac{\partial G^{(n)}}{\partial \rho} - (\gamma^2 \rho^2 + n^2) G^{(n)} = 0, \quad \dots (2.13)$$

where $\gamma = (\alpha^2 - k^2)^{1/2}$ is such that $\gamma = -ik$ when $\alpha = 0$, with branch cuts from ik to infinity that do not cross the strip (2.11). The modified Bessel functions $K_n(\gamma\rho)$ and $I_n(\gamma\rho)$ form an independent pair of solutions of (2.13), so that $G^{(n)}(\rho, \alpha)$ is the linear combination of these functions that satisfies the radiation requirements, the boundary condition (2.7) and ensures the regularity of $G^{(n)}(\rho, z)$ on the axis $\rho = 0$ and for $\rho = a, z > 0$. By the standard Wiener-Hopf procedure, this leads to the solution

$$G^{(n)}(\rho, \alpha) = \gamma a D_-(\alpha) \begin{cases} K'_n(\gamma a) I_n(\gamma \rho) & \text{if } \rho < a \\ I'_n(\gamma a) K_n(\gamma \rho) & \text{if } \rho > a \end{cases} \quad \dots (2.14)$$

$$\text{where } D_-(\alpha) = \left[G^{(n)}(\rho, \alpha) \right]_{\rho=a-0}^{a+0} = \int_{-\infty}^0 \left[G^{(n)}(\rho, z) \right]_{\rho=a-0}^{a+0} e^{i\alpha z} dz \quad \dots (2.15)$$

is the transform of the potential discontinuity.

The function $D_-(\alpha)$ is to be determined from the Wiener-Hopf equation

$$\gamma^2 a I'_n(\gamma a) K'_n(\gamma a) D_-(\alpha) = \frac{\partial G^{(n)}}{\partial \rho}(a, \alpha) + (-1)^n \frac{i^{n+1} 2\pi k \sin \theta_0 J'_n(ka \sin \theta_0)}{\alpha - k \cos \theta_0}, \quad \dots (2.16)$$

valid within the strip (2.11), where J_n is a Bessel function.

Defining the kernel

$$K^{(n)}(\alpha) = -2 K'_n(\gamma a) I'_n(\gamma a), \quad \dots (2.17)$$

the solution of (2.16) rests on the decomposition of K , which is analytic within the strip (2.11), as a product of 'plus' and 'minus' functions

$$K^{(n)}_+$$

$K_+^{(n)}$ and $K_-^{(n)}$ that are to be analytic and have no zeros in the respective regions $\text{im } \alpha > -k_0$ and $\text{im } \alpha < k_0$,

i.e.
$$K^{(n)}(\alpha) = K_+^{(n)}(\alpha) K_-^{(n)}(\alpha). \quad \dots (2.18)$$

In terms of these functions, described in Section 4, the standard Wiener-Hopf procedure leads to the solution

$$D_-^{(n)}(\alpha) = \frac{4\pi (-i)^{n+1} \sin \theta_0 J_n'(ka \sin \theta_0)}{a(1 + \cos \theta_0) K_+^{(n)}(k \cos \theta_0)} \frac{1}{(\alpha - k \cos \theta_0)(\alpha - k) K_-^{(n)}(\alpha)} \quad \dots (2.19)$$

This formula for $D_-^{(n)}(\alpha)$, together with (2.14) and (2.12), completes the formal solution for the function $G^{(n)}(\rho, z)$.

3. Solution for Sources near the Edge

The formal solution of Section 2 can be estimated in simpler forms in the asymptotic limits of high wave number ($ka \gg 1$) and low wave number ($ka \ll 1$). For high wave numbers the usual ray theory arguments predict that the potential at points in the vicinity of the edge will behave as if the scatterer were a flat semi-infinite plate, for which the results are already known. Thus our attention is directed to the case of waves of length large compared with radius, whence $ka \ll 1$.

It is instructive firstly to examine the form of the potential G at points very close to the lip of the pipe. For the incompressible nature of the flow in this vicinity implies a solution of the form

$$G \sim AC(\theta_0, \psi - \psi_0; k, a) \delta^{1/2} \sin \frac{1}{2} \omega + D(\psi - \psi_0) \quad \dots (3.1)$$

for $k\delta \ll ka \ll 1$, where δ, ω are polar co-ordinates based on the edge in a plane $\psi = \text{constant}$ (Fig. 2)

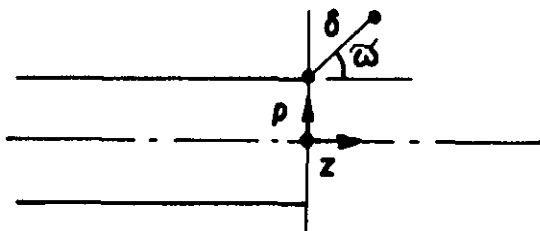


Fig. 2 Showing the co-ordinates (δ, ω) in the plane $\psi = \text{constant}$.

Thus the n^{th} Fourier component $G^{(n)}$ of G has the form

$$G^{(n)} \sim C^{(n)}(\theta_0; k, a) \delta^{1/2} \sin \frac{1}{2} \omega + D^{(n)}(\theta_0; ka) \quad \dots (3.2)$$

where/

where the scale function $C^{(n)}$ has the dimension $(\text{length})^{-1/2}$ to be formed from the pair of parameters k and a . The value of the constant $D^{(n)} = G^{(n)}(0,0)$ is of little interest; it can be calculated from the solution (2.12, 2.14), with $\rho = z = 0$, and is found to be of order ka for the modes $n = 0$ and $n = 1$, negligibly small for the other modes.

The form of the result (3.1) is common to all rigid bodies with a sharp edge; in particular, the single semi-infinite plate has no length scale a associated with its geometry so that the potential must assume the form $(k\delta)^{1/2} \sin \frac{1}{2} \omega$, as is already established by Ffowcs Williams and Hall (1970), Crighton and Leppington (1971).

To determine the form of the scale function $C^{(n)}(\theta_0; k, a)$ in the present case, we note that the discontinuity of potential, given according to formula (3.2) as

$$G^{(n)}(a + 0, z) - G^{(n)}(a - 0, z) \sim 2 C^{(n)}(-z)^{1/2}, \quad z < 0, \quad \dots (3.3)$$

has the Fourier transform $D_{-}^{(n)}(\alpha)$ that is given by an Abelian theorem (see Noble (1958)) as

$$\begin{aligned} D_{-}^{(n)}(\alpha) &= \int_{-\infty}^0 \left[G^{(n)}(\rho, z) \right]_{\rho=0}^{a+0} e^{i\alpha z} dz \\ &\sim \int_{-\infty}^0 2 C^{(n)}(-z)^{1/2} e^{i\alpha z} dz \quad \text{as } |\alpha| \rightarrow \infty. \end{aligned}$$

i.e.
$$D_{-}^{(n)}(\alpha) \sim C^{(n)} \pi^{1/2} (i\alpha)^{-3/2} \quad \text{as } |\alpha| \rightarrow \infty, \quad \text{im } \alpha > 0, \quad \dots (3.4)$$

with $D_{-}^{(n)}(\alpha)$ given exactly by formula (2.19).

Now it is shown in Section 4 that

$$K_{-}^{(n)}(\alpha) \sim (i\alpha a)^{-1/2} \quad \text{as } |\alpha| \rightarrow \infty, \quad \text{im } \alpha > 0,$$

so that the function $D_{-}^{(n)}(\alpha)$ of (2.19) is given asymptotically by

$$D_{-}^{(n)} \sim - \frac{4\pi (-i)^{n+1} \sin \theta_0}{a^{1/2} (1 + \cos \theta_0)} \frac{J_n'(ka \sin \theta_0)}{K_+^{(n)}(k \cos \theta_0)} (i\alpha)^{-3/2},$$

$$\text{as } |\alpha| \rightarrow \infty,$$

and/

and a comparison with formula (3.4) implies that

$$c^{(n)} = - \frac{4\pi^{1/2} (-i)^{n+1} \sin \theta_0}{a^{1/2} (1 + \cos \theta_0)} \frac{J'_n(ka \sin \theta_0)}{K_+^{(n)}(k \cos \theta_0)} \dots (3.5)$$

This formula can be simplified in the long wave limit $ka \ll 1$, by using the asymptotic estimates (4.16, 4.17) for $K_+^{(n)}(k \cos \theta_0)$ and by replacing the Bessel function J'_n by its small argument approximation. Thus we get

$$c^{(0)} \sim - 2i\pi^{1/2} ka^{1/2} (1 - \cos \theta_0) \dots (3.6)$$

and
$$c^{(n)} \sim \frac{4\pi^{1/2} (-i/2)^n (ka \sin \theta_0)^n}{n^{1/2} (n-1)! a^{1/2}}, \quad n \geq 1, \quad \text{as } ka \rightarrow 0. \dots (3.7)$$

We note that the zeroth and first modes are of order ka , the higher modes $n \geq 2$ being negligible for small ka . Retaining these terms only, we see from (3.2) and (2.8) that G is given by

$$G(\underline{x}; \underline{x}_0) \sim -i\pi^{-1/2} ka^{1/2} \delta^{1/2} \sin \frac{1}{2} \varpi \frac{e^{ik|\underline{x}_0|}}{|\underline{x}_0|} \left\{ (1 - \cos \theta_0) + 2 \sin \theta_0 \cos(\psi - \psi_0) \right\}, \dots (3.8)$$

for $k|\underline{x}_0| \gg 1$, $k\delta \ll ka \ll 1$, together with a term of the same order, independent of (δ, ϖ) arising from the term $D^{(n)}$ of (3.2).

The far field estimate (3.8) is valid only for sources that are very close to the end, with $\delta \ll$ radius a , and it is important to deal with the extended region that is close to the end on a wavelength scale, but with δ/a either large or small.

To calculate the nature of the field within a wavelength of the end, we need a uniform estimate for the function $(a - k \cos \theta_0)(a - k) K_-^{(n)}(\alpha)$ appearing in (2.19), with $|a|$ large compared with k , but with $a\bar{a}$ arbitrary. It is clear that $(a - k \cos \theta_0)(a - k) \sim a^2$ for $|a| \gg k$, and the estimate

$$\log K_-^{(n)}(\alpha) \sim \frac{iaa}{\pi} \int_0^\infty \frac{\log(-2 K'_n(x) I'_n(x)) dx}{x^2 + (iaa)^2} \equiv \log \hat{K}_-^{(n)}(\alpha) \dots (3.9)$$

is calculated in Section 4. The detailed form of (3.9) is not crucial, but it is important to note that the uniform estimate $K \sim \hat{K}$ is independent of the wave number k . It follows immediately that the k -dependence of the potential $G^{(n)}$ arises only through the multiplicative factor

$$\left\{ \frac{J'_n}{K_+^{(n)}} \right\}$$

$\left\{ J'_n(ka \cos \theta_0) / K_+^{(n)} k \cos \theta_0 \right\}$ of (2.19), and is therefore preserved unaltered from the region $\delta \ll a$ described by formula (3.8) to the extended region $\delta \ll 1/k$ contained within a wavelength from the end. Thus (3.8) can be generalised to give an estimate of the form

$$G(\underline{x}; \underline{x}_0) \sim ka \frac{e^{ik|\underline{x}_0|}}{|\underline{x}_0|} \left\{ F_0(\rho/a, z)(1 - \cos \theta_0) + F_1(\rho/a, z) \sin \theta_0 \cos(\psi - \psi_0) \right\} \quad \dots (3.10)$$

for $k|\underline{x}_0| \gg 1$, $k|\underline{x}| \ll 1$. The functions F_0 and $F_1 \cos(\psi - \psi_0)$ are harmonic functions, independent of wavelength; their precise form is not of particular importance, but they can readily be expressed exactly in terms of a Fourier integral that involves the function $\hat{K}_-^{(n)}(\alpha)$ of (3.9).

The corresponding result for a distribution of quadrupoles of incident field

$$\phi_i(\underline{x}_0) = \int Q_{ij} \frac{\partial^2}{\partial x_i \partial x_j} \frac{e^{ik|\underline{x}-x_0|}}{|\underline{x}-x_0|} d\underline{x} \quad \dots (3.11)$$

is given by direct superposition as

$$\phi(\underline{x}_0) \sim ka \frac{e^{ik|\underline{x}_0|}}{|\underline{x}_0|} \left\{ P_0(1 - \cos \theta_0) + P_1 \sin \theta_0 \right\}, \quad \dots (3.12)$$

where $P_0 = \int Q_{ij} \frac{\partial^2 F_0}{\partial x_i \partial x_j} d\underline{x}$, $P_1 = \int Q_{ij} \frac{\partial^2}{\partial x_i \partial x_j} (F_1 \cos(\psi - \psi_0)) d\underline{x}$.

It is seen therefore that the ratio of the far field potential ϕ against that of the incident potential ϕ_i is given by

$$\left| \phi / \phi_i \right| = O((ka)^{-1}). \quad \dots (3.13)$$

Formula (3.13) should be contrasted with the corresponding result for sources within a distance r_1 from the edge of a semi-infinite plate, for which

$$\left| \phi / \phi_i \right| = O((kr_1)^{-1/2}) \quad \dots (3.14)$$

Evidently/

Evidently a sharp ended pipe is not so efficient as the half-plane for enhancing the sound field of quadrupole sources. Indeed, the results for the pipe are very closely analogous to those for scattering by a small finite body.

4. Properties of the Wiener-Hopf Factorisation Functions

The kernel $K(\alpha)$ of the Wiener-Hopf equation is defined as

$$K^{(n)}(\alpha) = -2 K'_n(\gamma a) I'_n(\gamma a), \quad \dots (4.1)$$

where K_n, I_n are modified Bessel functions and $\gamma = (\alpha^2 - k^2)^{1/2}$. It can be shown (Levine and Schwinger (1948), Jones (1955), Noble (1958)) that $K^{(n)}(\alpha)$ is analytic and has no zeros within the strip

$$-k_2 < \text{im } \alpha < k_2, \quad k_2 = \text{im } k, \quad \dots (4.2)$$

and it is required to factorise K in the form

$$K^{(n)}(\alpha) = K_+^{(n)}(\alpha) K_-^{(n)}(\alpha), \quad \dots (4.3)$$

where $K_+^{(n)}$ and $K_-^{(n)}$ are analytic and have no zeros in the respective regions $\text{im } \alpha > -k_2, \text{im } \alpha < k_2$.

Following the usual procedure of expressing $\log K(\alpha) = \log K_+ + \log K_-$ by the Cauchy formula, it is found that

$$\log K_{\pm}^{(n)}(\alpha) = \frac{\pm 1}{2\pi i} \int_{-\infty \mp ib}^{\infty \mp ib} \frac{\log \{-2K'_n((t^2 - k^2)^{1/2} a) I'_n((t^2 - k^2)^{1/2} a)\}}{t - \alpha} dt, \quad \dots (4.4)$$

$\mp \text{im } \alpha < b < k_2$

with the integrals interpreted as principal values, $\lim_{N \rightarrow \infty} \int_{-N \mp ib}^{+N \mp ib} dt$.

(i) Asymptotic evaluation of $K_-^{(n)}(\alpha)$ for large $|\alpha|$

Following the method due to Levine and Schwinger (1948), we take b to be zero, with $k_2 \rightarrow 0$, whence

$$\begin{aligned} \log K_{-}^{(n)}(\alpha) &= - \frac{\alpha}{\pi i} \int_0^k \frac{\log \{ \pi i H_n'((k^2 - t^2)^{1/2} a) J_n'((k^2 - t^2)^{1/2} a) \}}{t^2 - \alpha^2} dt \\ &\quad - \frac{\alpha}{\pi i} \int_k^\infty \frac{\log \{ -2K_n'((t^2 - k^2)^{1/2} a) I_n'((t^2 - k^2)^{1/2} a) \}}{t^2 - \alpha^2} dt, \end{aligned} \quad \dots (4.5)$$

where H_n is the Hankel function of the first kind

$$\begin{aligned} &= - \frac{\alpha}{\pi i} \int_0^{ka} \frac{\log \{ \pi i H_n'(x) J_n'(x) \} x dx}{\left(k^2 - \frac{x^2}{a^2} - \alpha^2\right) (k^2 a^2 - x^2)^{1/2}} \\ &\quad - \frac{\alpha}{\pi i} \int_0^\infty \frac{\log \{ -2K_n'(x) I_n'(x) (k^2 a^2 + x^2)^{1/2} \} x dx}{\left(k^2 + \frac{x^2}{a^2} - \alpha^2\right) (k^2 a^2 + x^2)^{1/2}} \\ &\quad - \frac{1}{\pi} \int_{ka/ia}^\infty \frac{\log(iaa x)}{x^2 + 1} dx \end{aligned} \quad \dots (4.6)$$

$$\approx O(\alpha^{-2}) + O(\alpha^{-1}) - \frac{1}{2} \log(iaa) \text{ as } |\alpha| \rightarrow \infty.$$

Thus $K_{-}^{(n)}(\alpha) \sim (iaa)^{-1/2}$ as $|\alpha| \rightarrow \infty$, in $\alpha < 0$. $\dots (4.7)$

The estimate (4.7) holds as $|\alpha| \rightarrow \infty$, with $|\alpha| \gg k$ and $|\alpha| \gg 1/a$. More generally, a calculation of the potential field within a wavelength from the end of the pipe requires a uniform asymptotic estimate for $|\alpha| \gg k$, $ka \ll 1$, but with $|a\alpha|$ arbitrary.

The first integral of (4.5) is found again to be negligibly small, while the remaining integral is given by

$$- \frac{\alpha}{\pi i} \int_0^\infty \frac{\log \{ -2K_n'(x) I_n'(x) \} x dx}{(k^2 a^2 + x^2)^{1/2} \left(k^2 + \frac{x^2}{a^2} - \alpha^2\right)} \sim - \frac{aa}{\pi i} \int_0^\infty \frac{\log \{ -2K_n'(x) I_n'(x) \} x dx}{(k^2 a^2 + x^2)^{1/2} (x^2 - a^2 \alpha^2)}$$

for $|\alpha| \gg k$. Divide the range of integration at the point $x = \epsilon$, where ϵ is a small number such that $ka \ll \epsilon \ll a|\alpha|$. If x is less than ϵ it is much less than $a|\alpha|$, so that the factor $x^2 - a^2 \alpha^2$ can be replaced by $-a^2 \alpha^2$, and the function $-2K_n'(x) I_n'(x)$ can be

replaced/

replaced by its asymptotic form n/x^2 . For $x > \epsilon$, on the other hand, we may replace the radical $(k^2 a^2 + x^2)^{1/2}$ by x . It is found in this way that

$$\log K_{-}^{(n)}(\alpha) \sim \frac{i\alpha a}{\pi} \int_0^{\infty} \frac{\log(-2K_n'(x) I_n'(x))}{x^2 + (i\alpha a)^2} dx, \quad \dots (4.8)$$

for $|\alpha| \gg k$, $ka \ll 1$, with $\text{im } \alpha < 0$.

It is important to note that this estimate for $K_{-}^{(n)}(\alpha)$ is independent of the wave number k . For $|\alpha a| \gg 1$, it is easy to verify that the simpler result (4.7) is recovered from (4.8).

(ii) Asymptotic evaluation of the function $K_{+}^{(n)}(k \cos \theta_0)$

We require an estimate for the function $K_{+}^{(n)}(k \cos \theta_0)$ when ka is small. If the integral (4.4) is evaluated along the real axis with k real, then the limit $\alpha \rightarrow k \cos \theta_0$, with $\text{im } \alpha > 0$, requires the path of integration to be indented below the pole $t = k \cos \theta_0$. This indentation contributes πi times the residue at $k \cos \theta_0$, so that (4.4) leads to the result

$$\log K_{+}^{(n)}(k \cos \theta_0) = \frac{1}{2} \log \left\{ \pi i H_n'(ka \sin \theta_0) J_n'(ka \sin \theta_0) \right\} + \frac{ka \cos \theta_0}{\pi i} I^{(n)}, \quad \dots (4.9)$$

where
$$I^{(n)} = \int_0^{\infty} \frac{\log \{-2 K_n'(x) I_n'(x)\} x dx}{(k^2 a^2 \sin^2 \theta_0 + x^2)(k^2 a^2 + x^2)^{1/2}} + \int_0^{ka} \frac{\log \{\pi i H_n'(x) J_n'(x)\} x dx}{(k^2 a^2 \sin^2 \theta_0 - x^2)(k^2 a^2 - x^2)^{1/2}}, \quad \dots (4.10)$$

and \int_0^{ka} denotes a Cauchy principal value integral.

For small values of ka , we have

$$\pi i H_n'(ka \sin \theta_0) J_n'(ka \sin \theta_0) \sim \begin{cases} 1 & \text{if } n = 0 \\ n/(-ika \sin \theta_0)^2 & \text{if } n \geq 1 \end{cases} \quad \dots (4.11)$$

To deal with the integral $I^{(n)}$, note that the functions appearing in the logarithms have the small argument asymptotics

$$-2 K'_0(x) I'_0(x) = 1 + O(x^2 \log x), \quad \pi i H'_0(x) J'_0(x) = 1 + O(x^2 \log x); \quad \dots (4.12)$$

$$-2 K'_n(x) I'_n(x) = \frac{n}{x^2} \left(1 + O(x^2 \log x) \right), \quad \pi i H'_n(x) J'_n(x) \\ = - \frac{n}{x^2} \left(1 + O(x^2 \log x) \right) \quad \dots (4.13)$$

for $n \geq 1$. Letting $ka \rightarrow 0$ in formula (4.10), we have for $n = 0$,

$$I^{(0)} \sim \int_0^\infty \log \left\{ -2 K'_0(x) I'_0(x) \right\} \frac{dx}{x^2} \quad \text{as } \varepsilon \rightarrow 0. \quad \dots (4.14)$$

For $n \geq 1$, we may not simply replace ka by zero in the integrands, on account of convergence difficulties at the origin; this difficulty is readily overcome by inserting and subtracting suitably compensating logarithmic functions, dictated by (4.13). Thus for $n \geq 1$,

$$I^{(n)} = \int_0^\infty \frac{\log \{-2 K'_n(x) I'_n(x) x^2\} x dx}{(k^2 a^2 \sin^2 \theta_0 + x^2)(k^2 a^2 - x^2)^{1/2}} + \int_0^{ka} \frac{\log \{\pi i H'_n(x) J'_n(x) (-x^2)\} x dx}{(k^2 a^2 \sin^2 \theta_0 - x^2)(k^2 a^2 - x^2)^{1/2}} \\ - \int_0^\infty \frac{\log(x^2) x dx}{(k^2 a^2 \sin^2 \theta_0 + x^2)(k^2 a^2 - x^2)^{1/2}} - \int_0^{ka} \frac{\log(-ix)^2 x dx}{(k^2 a^2 \sin^2 \theta_0 - x^2)(k^2 a^2 - x^2)^{1/2}}.$$

Now as $ka \rightarrow 0$, the first two terms tend to constants; the remaining integrals can be evaluated exactly to give

$$I^{(n)} = \frac{i\pi}{ka} \sec \theta_0 \log \left(\tan \frac{1}{2} \theta_0 \right) + O(1) \quad \text{as } ka \rightarrow 0 \quad \dots (4.15)$$

Finally then, (4.9) and (4.11) show that

$$K_+^{(0)}(k \cos \theta_0) \sim 1 \quad \text{as } ka \rightarrow 0, \quad \dots (4.16)$$

$$\text{and } \log K_+^{(n)}(k \cos \theta_0) \sim \frac{1}{2} \log \frac{n}{(-ika \sin \theta_0)^2} + \log \left(\tan \frac{1}{2} \theta_0 \right), \quad n \geq 1,$$

i.e./

$$\text{i.e. } K_+^{(n)}(k \cos \theta_0) \sim \frac{i}{ka} \frac{n^{1/2}}{1 + \cos \theta_0} \quad \text{as } ka \rightarrow 0, \quad n \geq 1. \quad \dots (4.17)$$

5. Conclusion

The distant sound field induced by a quadrupole source distribution, within about a wavelength from the pipe exit, has the form

$$|\phi/\phi_i| = O((ka)^{-1}), \quad \text{for } ka \ll 1. \quad \dots (5.1)$$

To interpret this within the aerodynamic noise context, we make the crude identification $k \approx U/\ell c$ for the wave number, in terms of a typical turbulence velocity U and length scale ℓ associated with the turbulence, with c the wave speed. Thus the ratio of potentials is $|\phi/\phi_i| = O(\ell/Ma)$, where $M = U/c$ is a turbulence Mach number that is typically very small. Since the sound intensity is proportional to the square of the potential, the 'U⁶ law' of Lighthill is modified to give dependence $I \propto U^6$ that is generally applicable to small finite bodies.

Although this represents a large increase in sound, compared with that due to the incident field alone, it is less than that scattered by the sharp edge of either a single semi-infinite plate or a parallel pair of such plates. For these geometries it has been found that $|\phi/\phi_i| = O((ka)^{-3/2})$ whence $I \propto U^8$. It is perhaps surprising that the scattering property of the sharp ended pipe resembles that of a finite body rather than that of the parallel half-planes.

References

- | | |
|---|--|
| D. G. Crighton and
F. G. Leppington | J. Fluid Mech. <u>46</u> , 577. 1971. |
| N. Curle | Proc. Roy. Soc. <u>A.231</u> , 505. 1955. |
| J. E. Ffowcs Williams and
L. H. Hall | J. Fluid Mech. <u>40</u> , 657. 1970. |
| D. S. Jones | Phil. Trans Roy. Soc. <u>A.247</u> , 499. 1955. |
| H. Levine and
J. Schwinger | Phys. Rev. <u>73</u> , 383. 1948. |
| M. J. Lighthill | Proc. Roy. Soc. <u>A.211</u> , 566. 1952. |
| B. Noble | Methods based on the Wiener-Hopf technique.
Pergamon. 1958. |

Chapter 6

Conclusions

The jet noise that we are now considering is increasingly important at the lower jet velocities and is most significant at high angles to the jet axis. It scales with a velocity index distinctly less than 8 and probably less than 6. This noise seems to exist at frequencies that are characteristically higher than those usual for jet noise. The evidence on which these conclusions are based is largely heresay in the context of modern engines but is fully consistent with the early measurements on the first generation of commercial jet engines (Mawardi and Dyer 1952). We are now inclined to regard the noise radiated normal to the jet axis in the one direction unaffected by Doppler frequency shifts and where non-Lighthillian behaviour is common experience (Lighthill 1961), as a different noise in the category of the low speed problem. We think it is not a Reynolds and/or Mach number effect that modifies the free turbulence sound. This low speed behaviour at the high angles is continued to supersonic jet speeds, so that the phenomenon is not exclusively a low speed problem. The noise velocity index is, we think, likely to prove a good diagnostic tool, since we do not believe that there are likely to be significant subtle Mach number, Reynolds number and geometric changes that will so cloud the picture that it defies a proper modelling. The dependence of noise on the very low powers of velocity (from 2-6) that are reported indicate to us, completely unambiguously, that the noise sources must arise from a mechanism that is fundamentally more efficient in generating sound than Lighthill's free quadrupole mechanism. This new and important mechanism is probably still described by Lighthill's quadrupole acoustic analogy, but boundary constraints must be imposed to attain high radiation efficiency. These constraints must be either at or within the nozzle exit. We have examined what increase in the radiation can result from an interaction of aerodynamic sources with boundary constraints of the type met in a jet engine exhaust system. The problem falls naturally into two categories according to whether the radiated wavelength is large or small on the nozzle scale. Consider first the long wave problem.

1. The long wave problem

Acoustic frequencies are identical to source frequencies. Aerodynamic sources have frequencies set on a Strouhal scale \underline{U}/ℓ , U and ℓ being the characteristic velocity and length scale of the source flow. The acoustic wavelength, λ , radiated by this flow is $\lambda = \ell (MS)^{-1}$ where M and S are the Mach and Strouhal numbers respectively. The long wavelength condition is then precisely defined by the inequality

$$\frac{\lambda}{D} \gg 1 \quad \text{or} \quad \frac{D}{\ell} MS \ll 1, \quad D \text{ being the jet diameter.} \quad \text{In this limit the}$$

containment of the sources deep within the pipe will increase their ability to generate sound. However that sound cannot propagate in one attempt through the nozzle. It is mostly reflected upstream. If it is redeflected downstream then in many attempts, as it were, the sound will eventually escape but only at the period determined by the time required for sound to travel from the nozzle upstream to a reflector and back again to the nozzle, i.e. the sound will exist at harmonics of the organ pipe frequency. Away

from/

from these pipe resonances the containment of aerodynamic sources deep inside the pipe cannot increase their ability to radiate sound to the pipe exterior. There is only one qualification to this. The nozzle contraction area ratio is assumed to be smaller than about 20. At very high nozzle contraction ratios the velocity index of aerodynamic sound generated deep inside the jet pipe will be reduced by 2. Turbulence and unsteady blade forces will therefore radiate sound in proportion to U^6 and U^4 respectively. In this limit that has, as far as we can see, no immediate practical interest aerodynamic sources in the vicinity of the nozzle exit plane radiates sound more effectively. Also, even for small nozzle contraction ratios, quadrupole sound generated at the nozzle exit plane will scale on the sixth power of velocity and dipole sound on the fourth power.

2. The short wave problem $MS D/\ell \gg 1$

This limit is the one of immediate practical concern because jet diameters are now so large that the annoying sounds have relatively short wavelengths. We conclude in this limit again that the containment of aerodynamic sources in the jet pipe cannot fundamentally increase their radiating ability. Sound will propagate through the nozzle with great ease, the only real influence being on the directionality of the sound. The search for high efficiency sources must therefore concentrate on mechanisms of high efficiency in their own right and not rely on some subtle interaction between boundary effects that are more than a wavelength from the source. We identify two mechanisms of high acoustic efficiency and which are likely source mechanisms for the low speed high frequency problem.

2a. Helmholtz resonator sound

Within an engine there are resonant chambers or cavities that constitute resonators of the Helmholtz type. When these cavities are driven by a turbulence field, or by turbulent combustion at frequencies above the resonance, then the scattered sound increases in proportion to the fourth power of velocity. There will also be resonance frequency sound increasing in proportion to the cube of velocity but the resonant band-width is likely to be very large and the resonant sound non-discrete. The frequency of this sound will be determined by the frequencies of turbulence in the environment of the resonator opening. This mechanism could easily be examined experimentally. A combustion chamber could be tested in isolation to discover first its acoustic characteristics and secondly its sound scattering ability. The turbulence could be generated by a cold turbulent air jet exhausting into the interior of the chamber. Within an engine the pressure fluctuation within the combustion chamber would correlate with the radiated sound if this mechanism is dominant.

2b. Edge scattered sound

High frequency sound generated within a wavelength of the nozzle periphery is a possible source mechanism of great importance. The scattered field intensity increases with a velocity index equal to or less than 5. The radiated frequencies are higher than those in conventional jet noise by a factor U/u' , U being the mean jet velocity and u' the root mean square turbulence level in the vicinity of the edge. The edge scattered field radiates preferentially away from the jet axis. The edge can convert into sound, by a diffraction process, the local hydrodynamic motion of a slowly

evolving/

evolving eddy such as, for example, a torroidal vortex that is convected with the stream. The energy scattered from a single eddy during low speed convective motion past an edge increases in proportion to $\frac{\rho U^4 \ell^6}{c^2 d^3} \rho$

being the fluid density, U the mean stream velocity, ℓ the characteristic eddy scale and d the nearest distance to which the eddy approaches the edge. In a continuous turbulent flow eddies will arrive at a frequency

U
- to be scattered with the above efficiency so that the rate at which energy ℓ is scattered, or the acoustic power level, is proportional to $\rho U^5 \frac{\ell^5}{c^2 d^3}$.

This re-emphasises the conclusion reached by Ffowcs Williams and Hall (1970) in a formal solution of Lighthill's equation. We have examined also the rôle played by the shear layer evolving from a nozzle lip, and whether a Kutta constraint should be imposed on the motion, and what effects such a constraint would have on the sound field. This is the problem treated in great detail in Chapter 3. Our main conclusions are that radiation of shear layer instabilities can be affected by the scattering edge and that the effect is more pronounced when some Kutta constraint is active. We conclude that the edge region, and the instabilities of the early shear layer, are likely to be of substantial importance to the lower speed jet noise problem at high frequencies. Experimentally this aspect could be checked in several ways. The edge geometry could be changed. The bounding surfaces could be lagged to make them appear compliant. The shear layer mean velocity profile could be controlled by edge suction, or blowing, or vortex generators or swirl producers, to modify the instability modes that are evidently scattered with high efficiency.

Finally, there are several aspects of the problem that remain unresolved and where further theoretical work should be encouraged. These concern the influence of shear layer curvature and the basic interaction of the cylindrical shear layer with its nozzle. The question of how to limit the exponential growth of instabilities is also only plausibly dealt with at present and the whole issue of determining details of the internal engine acoustics in the presence of mean flow is wide open. What we have done here is to point out that these internal characteristics can be the controlling features of the low speed noise problem. Experimentally the field is also in its infancy. The experiments so far reported abound with the confusion that is inevitable while the likely physical processes remain unidentified. We would hope that these processes have become clearer as a result of this preliminary theoretical survey and that this report will enable the experimenter to make more rapid progress in the clear isolation and elimination of those excess noise sources that seem to be dominating the jet noise of the newer engines.

© *Crown copyright 1972*

Produced and published by
HER MAJESTY'S STATIONERY OFFICE

To be purchased from
49 High Holborn, London WC1V 6HB
13a Castle Street, Edinburgh EH2 3AR
109 St Mary Street, Cardiff CF1 1JW
Brazennose Street, Manchester M60 8AS
50 Fairfax Street, Bristol BS1 3DE
258 Broad Street, Birmingham B1 2HE
80 Chichester Street, Belfast BT1 4JY
or through booksellers

Printed in England